Journal of Experimental Marine Biology and Ecology 591 (2025) 152119

Contents lists available at ScienceDirect

Journal of Experimental Marine Biology and Ecology

journal homepage: www.elsevier.com/locate/jembe

Toxic impact of aluminium on the natural phytoplankton community during spring in the Atlantic sector of the Southern Ocean

C. Demasy [a,*], A. Singh [a,b,c], S. Samanta [a,d], T.J. Ryan-Keogh [c], A.N. Roychoudhury [a]

[a] Department of Earth Sciences, Stellenbosch University, Stellenbosch, South Africa
[b] Department of Chemistry, Norwegian University of Science and Technology, Trondheim, Norway
[c] Southern Ocean Carbon-Climate Observatory, CSIR, Cape Town, South Africa
[d] School of Geosciences, University of the Witwatersrand, Johannesburg, South Africa

ARTICLE INFO

Keywords:
Aluminium
Phytoplankton
Atlantic Southern Ocean
Photophysiology
Climate change

ABSTRACT

The natural Southern Ocean phytoplankton community plays a pivotal role in both the marine trophic chain and global climate regulation. Previous studies and models have primarily focused on the individual effects of iron (Fe) on phytoplankton, often overlooking the potential toxic impact of aluminium (Al) and its interactive effects with Fe and cobalt (Co). Here, a series of controlled incubations involving the addition of trace metals (Al, Fe, and Co) were conducted to evaluate the potential effects of these elements in the Polar Frontal Zone and the Marginal Ice Zone. The findings revealed that the introduction of 1 nM of Al prompted a reduction in biomass of the entire natural community, coupled with a decrease in the photosynthetic efficiency (F_v/F_m) and an increase of the absorption cross-section of photosystem II (σ_{PSII}). A similar toxic impact of Al addition was observed at both sites, however, the level of cell activity and presence of other micronutrients (Fe, Co) attenuated the toxicity to some extent. Despite its connotations, Al toxicity is not considered an immediate threat to the sub-Antarctic phytoplankton community, however, the scenario could differ in regions where increased lithogenic input is likely.

1. Introduction

The role of phytoplankton has been extensively studied in the Southern Ocean (SO) both as the foundation of the marine trophic web and its role in climate regulation (Deppeler and Davidson, 2017; Henley et al., 2020), converting the atmospheric carbon into organic matter, a fraction of which is subsequently sequestered to the ocean floor (Ducklow et al., 2001). Optimal physical and biogeochemical conditions are crucial for sustaining phytoplankton and to ensure photosynthesis enabling the transformation of this carbon into organic matter. The cornerstone of phytoplankton growth is optimal temperature, light, pH conditions and the availability of macronutrients and micronutrients (e.g. iron (Fe) and cobalt (Co)) (Boyd et al., 2016; Lohan and Tagliabue, 2018).

In the SO, the chemical composition of seawater is primarily controlled by lithogenic inputs stemming from erosion and sources such as dust, resuspended sediments, ice-melt, hydrothermal activities as well as internal cycling (Ardyna et al., 2019; Lannuzel et al., 2008; Mahowald et al., 2005; Tagliabue et al., 2018). In addition, these contributions vary depending on the biogeochemical regime of the SO (Deacon, 1982; Orsi et al., 1995; Park et al., 1993; Pollard et al., 2002). Consequently, distinct phytoplankton communities are observed within each zone (Eriksen et al., 2018; Viljoen et al., 2019; Wright et al., 2010). This study specifically is focused on two regions: the Polar Frontal Zone (PFZ) and the Marginal Ice Zone (MIZ) during the austral spring season. Notably, phytoplankton productivity in the SO exhibits seasonal and spatial variations (Arrigo et al., 2008; Moore and Abbott, 2000), characterized by the initiation of blooms, primarily occurring during the spring and summer when favourable growth conditions prevail such as prolonged daylight hours, increased light intensity, and the nutrient replenishment from the winter period (Rohr et al., 2017). The PFZ is characterized by strong seasonal changes in temperature and nutrients driven by phytoplankton dynamics, with spring blooms dominated by nano- and picophytoplankton (Flynn et al., 2023; Kopczyńska et al., 2007; Lourey and Trull, 2001; Thomalla et al., 2011). In contrast, the MIZ is recognized for its distinctive features, notably the expansion and contraction of ice formations around the continent (Vichi, 2022). Melting sea ice in spring releases essential nutrients into the water for phytoplankton (Johnson

* Corresponding author.
E-mail address: demasy@sun.ac.za (C. Demasy).

https://doi.org/10.1016/j.jembe.2025.152119
Received 29 October 2024; Received in revised form 27 June 2025; Accepted 3 July 2025

et al., 2023). However, light limitations prevail during this time due to deep mixing (Mitchell et al., 1991; Nelson and Smith, 1991), and grazing (Dubischar and Bathmann, 1997; Smetacek et al., 2004). Unlike the PFZ, blooms in the MIZ typically occur during the summer months (Thomalla et al., 2023; Thomalla et al., 2011), exhibiting substantial inter-annual and intra-seasonal variability in primary production within the SO (Smith et al., 1988). These seasonal and zonal differences in the phytoplankton community, therefore, have consequences for the rate of carbon uptake (Brzezinski et al., 2003; Deppeler and Davidson, 2017; Popp et al., 1999).

The majority of research concerning trace metals in the SO has traditionally emphasized their potential benefits, yet little attention has been paid to exploring whether lithogenic inputs could introduce toxic elements into phytoplankton. Indeed, certain metals in the marine environment have been associated with detrimental effects on phytoplankton metabolism. For instance, a variety of metals, including copper (Cu), lead (Pb), zinc (Zn), and cadmium (Cd), have been linked to toxicity for phytoplankton when the concentrations exceed threshold limits (Bilgrami and Kumar, 1997; Okamura and Aoyama, 1994). Moreover, the nature of these toxic effects might be contingent on the source of the metals. For instance, Paytan et al. (2009) demonstrated that input of Cu aerosol triggered toxicity for cyanobacteria. Similarly, the negative impacts of nanoparticles, such as titanium and Zn, were observed in two diatom species (Miller et al., 2010). Conversely, Al has predominantly been documented for its toxic properties in terrestrial environments, including soils and water bodies, and has exhibited adverse effects on aquatic organisms, plants, and human health (Botté et al., 2022; Gensemer and Playle, 1999; Macdonald and Martin, 1988; Rahman and Upadhyaya, 2021). However, limited research has addressed the impact of Al within marine ecosystems, and no studies have examined its role within the context of the SO.

Nonetheless, despite Al ranks being the third most abundant element in the Earth's crust (Wedepohl, 1995), the SO exhibits in general, low concentrations. Furthermore, Al is highly insoluble in oxygenated seawater, thereby accounting for the low dissolved Al (dAl) concentration in the water. However, in the PFZ, strong upwelling of deep water have been observed (Sokolov and Rintoul, 2007), input of Al from dust (220 and 470 pmol/m^3, Kangueehi, 2021) and Al concentrations as high as 3.28 nmol/L were detected due to island mass effect (Planquette et al., 2009). The recorded concentration of Al within the mixed layer ranged between 0.05 and 660.2 nmol/L (mean: 0.8 ± 0.9 nmol/L, $n = 61$) (Menzel Barraqueta et al., 2020; Middag et al., 2011). Additionally, the melting sea ice during spring contains high metal concentrations, including dAl (1.3–7.2 nmol/L) and particulate Al (0.4–142 nmol/L) as potential sources (Lannuzel et al., 2011) which could supply significant amount of Al to the MIZ. Furthermore, in the context of climate change, the input of metals into the SO is projected to increase (Henley et al., 2020). Consequently, these concentrations could potentially impact marine species, as Van Dam et al. (2018) reported a threshold limit of Al in seawater (2 μmol/L) to protect 95 % of the marine species.

In seawater, Al can exist in two distinct chemical forms: aluminate anion ($Al(OH)_4^-$) and aluminium hydroxide ($Al(OH)_3^0$) (Andrade and Costa Marques, 2012; Millero et al., 2009). However, the precise proportions among these chemical species remain undetermined, primarily due to the lack of a method capable of accurate measurement (Gillmore et al., 2016). Additionally, the uptake of Al into the marine trophic web is limited due to its low solubility in oxygenated and alkaline seawater (Gitelman, 1989). However, the concentrations observed in phytoplankton cells could be higher compared to other toxic metals such as Cu and Pb (Liu et al., 2019; Martin and Knauer, 1973).

The majority of studies on Al have primarily been centered on the scavenging effect exhibited by marine micro-organisms (e.g. Koning et al., 2007; Machill et al., 2013). These organisms have the capability to either adsorb Al onto their surfaces or absorb it within their cells, thereby reducing the Al concentration in seawater (Liu et al., 2019; Moran and Moore, 1988). Some studies have indicated a toxic impact of Al on certain phytoplankton groups (Gensemer and Playle, 1999; Gillmore et al., 2016; Saçan et al., 2007). A review even proposed the possibility of Al having a beneficial effect on growth, as posited by the Fe-Al hypothesis (Zhou et al., 2018b; Zhou et al., 2018a) and suggests that Al may enhance Fe utilization during chlorophyll biosynthesis by facilitating the superoxide-mediated reduction of Fe(III) to Fe(II) within cells (Zhou et al., 2024). Therefore, it is important to clarify that the precise biological effects and underlying mechanisms remain to be established.

Understanding the influence of Al on natural phytoplankton communities in the PFZ and MIZ of the Southern Ocean (SO) remains limited, particularly beyond the summer season (Armand et al., 2008; Gibberd et al., 2013; Le Moigne et al., 2013; Shramik et al., 2013). Within the framework of the two distinct biogeochemical zones, the associated environmental parameters could have repercussions not only on Al speciation but also on the metabolism of phytoplankton cells. This, in turn, could trigger synergistic and antagonistic effects, potentially altering the degree of Al toxicity. Additionally, phytoplankton could develop metabolic acclimatization processes in response to environmental stress, enhancing their resistance and resilience. However, these metabolic adaptations could vary based on the context of the state of the community. Thus, the response during a phytoplankton bloom might differ from that during periods of inactivity and low cell concentrations. To address this gap, we conducted ship-board short-term phytoplankton incubation experiments during the spring of 2019 in the PFZ and MIZ of the South Atlantic Sector during the Southern Ocean Seasonal Experiment Cycle (SCALE; https://scale.org.za/). While Fe and Co additions were tested for micronutrient limitation and co-limitation, Al was introduced at lower concentrations than in previous studies to evaluate potential toxicity and impacts on biological function. Then, this study focused on (1) identifying micronutrient limitation patterns, and (2) assessing Al toxicity on the overall and group-specific phytoplankton communities.

2. Material and methods

2.1. Sampling areas

During the SCALE Spring cruise of 2019 (12/10/2019–20/11/2019), seawater sampling and phytoplankton incubation were performed on the research vessel *S.A. Agulhas II*, which sailed along the Good Hope line (Vichi and Ryan-Keogh, 2019) in the Atlantic sector of the SO. In this study, seawater samples were collected from two distinct biogeochemical zones. Experiments 1 (2019/10/16) and 4 (2019/11/14) took place in the Polar Frontal Zone, while experiments 2 (2019/10/19) and 3 (2019/11/09) were conducted in the Marginal Ice Zone, (Fig. 1, Table 1).

All materials and sampling procedures adhered rigorously to trace metal-clean sampling guidelines (Cutter et al., 2017). The trace metal-clean seawater utilized for phytoplankton incubations was sampled through the deployment of a GEOTRACES compliant CTD rosette equipped with 24 × 12 L clean Teflon™ coated Go-Flo® bottles which were deployed on a Kevlar cable (General Oceanics, USA). Seawater samples were acquired at a recommended depth of 25 m for phytoplankton incubation (Ross et al., 2011a, 2011b). Additional CTD profile data (temperature, salinity, oxygen and fluorescence concentration) for each station were collected and are available in the supplementary information (Fig. 3). Subsequently, the seawater dedicated for phytoplankton incubations was randomly distributed into 1 L pre-cleaned Poly-Carbonate bottles (ThermoFisher Scientific Nalgene) which is within the range of volumes used for phytoplankton incubation experiments (Browning et al., 2021; Domingues et al., 2023; Ryan-Keogh et al., 2013). Each step of the handling procedures, ranging from seawater spiking for experimental treatments to incubation, was meticulously conducted within a certified class-100 clean container specifically designed for trace metal applications.

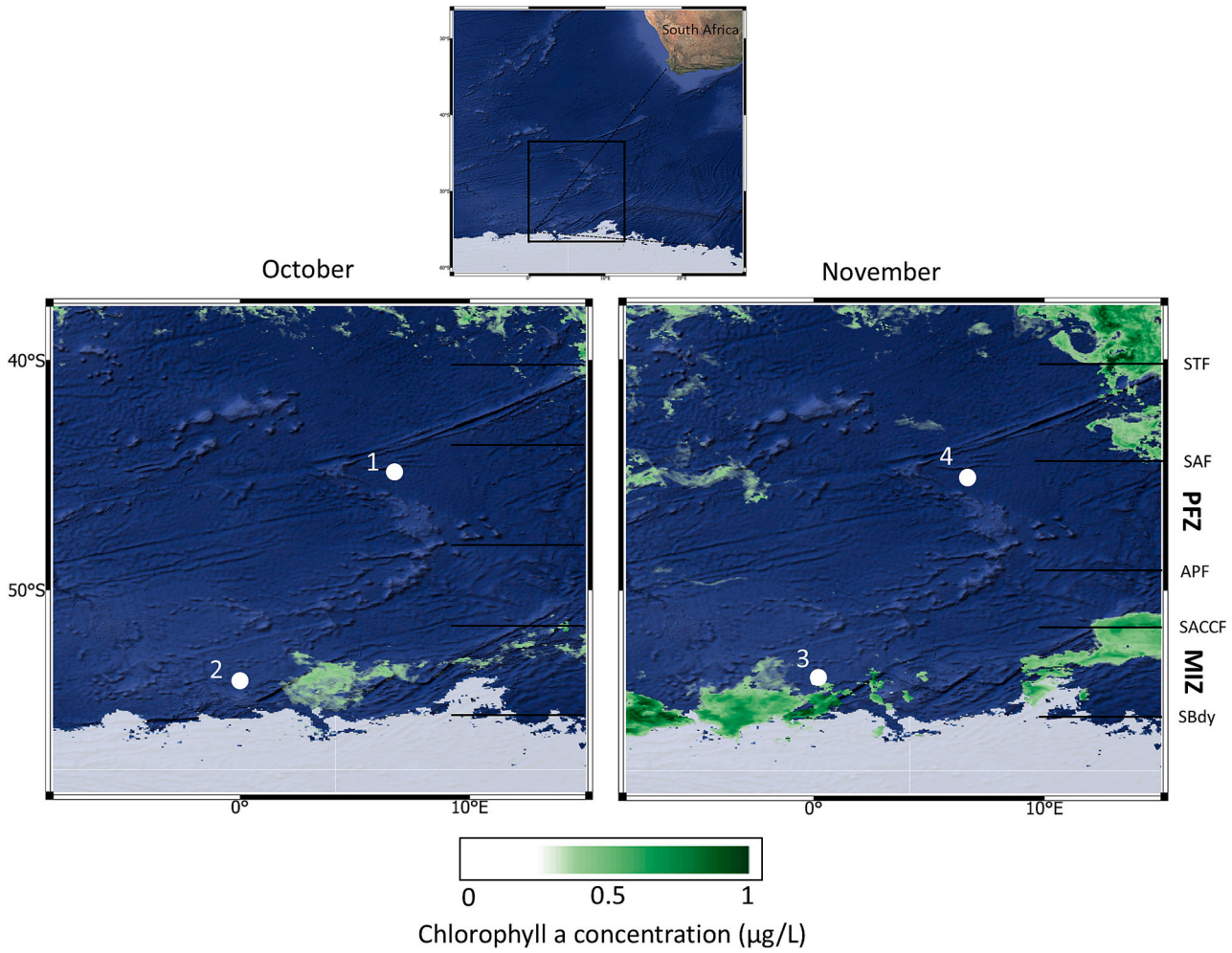

Fig. 1. Overview of the oceanographic cruise conducted in the Atlantic sector of the Southern Ocean (top), map indicating the locations of seawater sampling stations (1 and 2) in October, used for the phytoplankton incubation (left), and map showing seawater sampling stations (3 and 4) during November (right). The frontal position were mapped based on measurements of the temperature and salinity of water masses during the cruise (Deacon, 1982; Orsi et al., 1995; Park et al., 1993) including Sub-Tropical Front (STF), Sub-Antarctic Front (SAF), Antarctic Polar Front (APF), Circumpolar Current Front (SACCF) and Southern Boundary (SBdy). Chlorophyll *a* concentration were derived from Ocean Color (*NASA Ocean Biology Processing Group*, 2018) representing the average for October (16/10/2019 to 23/10/2019) and November (09/11/2019 to 16/11/2019). The sea ice cover was plotted using data at the date of 01/11/2019 (Spreen et al., 2008). Experiments 1 and 4 were conducted using seawater samples collected from the Polar Frontal Zone (PFZ), while in experiments 2 and 3 seawater from the Marginal Ice Zone (MIZ) were used.

Table 1
General and biogeochemical conditions in the initial seawater of the four experiments measured at 25 m depth.

Incubation	Experiment 1	Experiment 2	Experiment 3	Experiment 4
Date	16/10/2019	19/10/2019	09/11/2019	14/11/2019
Location	−45.000, 6.600	−54.007, −0.011	−54.000, 0.000	−44.999, 6.600
Biogeochemical zone	PFZ	MIZ	MIZ	PFZ
Depth (m)	25	25	25	25
Temperature (°C)	5.3	−0.4	−0.2	5.81
Salinity	33.94	34.09	34.10	34.18
pH	8.12	8.08	8.04	8.18
PAR (µmol m^{-2} s^{-1})	129	129	129	129
Daylight (hours)	11 h21	14 h03	15 h30	14 h44

2.2. Incubation of phytoplankton

The incubation bottles were sealed with parafilm and carefully placed inside double zip bags. To simulate the environmental conditions specific to each sampling station, the bottles were arranged randomly within a customized Minus40 Specialized Refrigeration™ incubator. The temperature was adjusted according to the conditions prevailing at the time of sampling, and the photosynthetically active radiation (PAR) was set to 129 µmol m^{-2} s^{-1} for all experiments (Table 1). Additionally, the duration of daylight exposure was tailored to correspond with the latitudinal and time zone characteristics of the respective stations. Before initiating each incubation experiment, a 1 L bottle was analyzed to establish the biogeochemical background at each station (referred to as the "initial" condition). Subsequently, each experiment was performed in triplicate, comprising the following treatments: a control with no addition of trace metals ("control"), an addition of only 1 nM Al ("Al"), an addition of 2 nM of Fe and 1 nM of Al ("FeAl"), and an addition of 2 nM of Fe and 1 nM of Co ("FeCo"). Fe, Al and Co solutions were made by diluting a mono-element standard solution (Fe: 1000 mg/L $FeCl_3$ standard, TraceCERT® Sigma-Aldrich; Al: 1002 mg/L Al standards, Inorganic Ventures® IV CGAL1; Co: 1000 mg/L Co standard,

TraceCERT® Sigma-Aldrich). The addition of metals did not alter the pH of the seawater, as the metals were introduced in two dilutions, leaving the residual acid concentration negligible relative to the overall seawater volume. The incubations were conducted on a short time scale, lasting 24 h, thereby minimizing the potential for alterations in biomass and preserving the natural phytoplankton community structure.

2.3. Macronutrients analysis

The background seawater, collected at a depth of 25 m, was stored in 50 mL Falcon tubes for measurement of macronutrient concentrations, including nitrate, silicate, and phosphate. Nitrate samples were preserved at −20 °C and analyzed within a span of 2–3 months after the cruise. This analysis was carried out using the Lachat QuikChem 8500 series 2 Flow Injection Autoanalyzer (FIA) (Egan, 2008) and the detection limit was 0.1 μM (Flynn et al., 2023). Phosphate and silicate concentrations were quantified directly onboard the vessel using colorimetry methods (Grasshoff et al., 1999; Parsons et al., 1984). A Thermo Scientific Genesis 30 Visible spectrophotometer was employed for these measurements, achieving detection limits of <0.1 μmol/L for phosphates and 0.05 μmol/L for silicates. All sample measurements were conducted in duplicate, with the accuracy and drift of the analyses systematically verified at the onset and end of the analysis, utilizing a certified reference material (SCOR-JAMSTEC CRMs) for quality control. Notably, the standard deviation of the samples was found to be 0.22 μmol/L for nitrates, 0.32 μmol/L for silicates, and 0.07 μmol/L for phosphates.

2.4. Trace metals analysis

Seawater for trace metal analysis was collected from pristine Go-Flo bottles. This seawater was subjected to filtration through Sartorius capsule filters (0.45 and 0.2 μm pore size filtration) using Tygon tubes, which had been thoroughly cleaned with high purity acid. To prevent contamination, a HEPA air-filter cartridge (HEPA-CAP/HEPA VENT, 75 mm, Whatman) was attached to the cylinder pressure valve. The filtered seawater was then transferred into LDPE Nalgene bottles, which had been meticulously cleaned following established protocols (Cutter et al., 2017). The samples were acidified to pH <2 using high-purity HCl (Ultrapur® Merck Chemicals). After acidification, the samples were double-bagged and stored at room temperature until analysis, which was carried out using a commercially available online ESI seaFAST S3 (Elemental Scientific®) system coupled with a quadrupole Inductively Coupled Plasma Mass Spectrometer (Agilent® Mass hunter 7900) (Samanta et al., 2021). The dFe blanks exhibited no detectable contamination, measuring at 0.050 ± 0.020 nmol/L, with a detection limit of 0.081 nmol/L, which were below the values recorded in the seawater background (Table 2). Reference seawater materials demonstrated strong agreement with certified values, with measured concentrations of 5.98 ± 0.10 nmol/L for NASS-7 (National Research Council, Ottawa, ON, Canada; certified: 6.16 ± 0.47 nmol/L), 0.21 ± 0.03 nmol/L for GSP-62 (GEOTRACES Pacific surface seawater; consensus: 0.16 ± 0.05 nmol/L), and 1.63 ± 0.10 nmol/L for GSC 1–19 (2009 GEOTRACES coastal surface seawater consensus: 1.54 ± 0.12 nmol/L). To monitor instrumental drift, an internal indium standard was used, revealing a drift of less than 20 % over time.

Table 2
Initial concentrations of macronutrients (NO_3, SiO_4, PO_4), dissolved trace metals (Mn, Fe, Cu, Zn, Co, Cd, and Pb) and the concentration of chlorophyll *a* in the 4 different experiments. NA is defined as not analyzed.

Background concentration	Experiment 1 (PFZ)	Experiment 2 (MIZ)	Experiment 3 (MIZ)	Experiment 4 (PFZ)
NO_3 (μmol/L)	24.60 ± 0.17	28.70 ± 0.11	27.31 ± 0.35	21.61 ± 0.32
SiO_4 (μmol/L)	7.35 ± 0.11	43.76 ± 0.19	40.19 ± 0.27	5.98 ± 0.12
PO_4 (μmol/L)	1.58 ± 0.00	1.92 ± 0.01	1.65 ± 0.10	1.50 ± 0.03
dMn (nmol/L)	NA	0.42 ± 0.01	0.41 ± 0.00	0.24 ± 0.01
dFe (nmol/L)	NA	0.82 ± 0.11	0.75 ± 0.03	0.30 ± 0.06
dCu (nmol/L)	NA	1.59 ± 0.01	1.59 ± 0.01	0.83 ± 0.01
dZn (nmol/L)	NA	3.00 ± 0.04	2.48 ± 0.04	0.52
dCo (pmol/L)	NA	32.70 ± 1.08	34.97 ± 0.04	29.42 ± 0.23
dCd (pmol/L)	NA	663 ± 4	627 ± 2	319.7 ± 0.8
dPb (pmol/L)	NA	5.60 ± 0.12	6.03 ± 0.17	8.22 ± 0.40
Chl *a* (μg/L)	0.42	0.33	1.06	0.84

2.5. Photophysiological fluorescence measurements

To investigate the impact of physiological stress on the photosynthetic system of phytoplankton, measurements of photochemical efficiency (F_v/F_m) and photosystem II effective absorption cross-section (σ_{PSII}) were conducted (Suggett et al., 2009). Prior to measurement, the samples were acclimated in darkness for a duration of 30 min to eliminate the influence of non-photochemical quenching (Roháček, 2002; Schuback et al., 2021). Subsequently, the measurements were carried out using Fast Repetition Rate fluorometry (FRRf), employing the FastOcean FRRf system (Chelsea Scientific Instruments Fasttrack-aTM Mk II FastOcean FRRf) in conjunction with a FastActTM laboratory system, featuring a flash saturation sequence (comprising 100 × 1 μs flashlets with a 2 μs interval). A blank correction was undertaken by passing the sample through a 0.2 μm filter using a syringe (Cullen and Davis, 2003). Excitation of the samples was achieved with a light-emitting diode at a wavelength of 450 nm, with adjustments made between samples to ensure saturation of the observed transients. Measurement data were recorded using the FastPro8 software (v1.0.55). Subsequent data processing was executed using the customized package Phytoplankton Photophysiology Utilities in Python 3.7 (Ryan-Keogh and Robinson, 2021). Specifically, a fluorescent light curve was generated for the initial condition, the control with the lowest F_v/F_m value, and the treatment sample with the highest F_v/F_m value. Key parameters including F_o (minimum fluorescence), F_m (maximum fluorescence), F_v/F_m, and σ_{PSII} were derived from the saturation phase of the model (Kolber et al., 1988) with a connectivity coefficient of 0.3 (Suggett et al., 2001). The photophysiology results were analyzed for their variance using an ANOVA and using a pairwise Tukey test (Fisher, 1992; Tukey, 1949).

2.6. Pigments measurements

A volume of 500 mL of seawater was filtered through a GF/F Whatman filter (0.7 μm, 25 mm) under low vacuum pressure (ca. -30 kPa). Two distinct analyses of pigment concentrations were undertaken. Firstly, the filters were directly measured onboard using fluorometry. Secondly, additional filters were preserved by storing them at −80 °C for HPLC analysis.

Initially, the determination of total chlorophyll *a* content was conducted in triplicate. Filters utilized in the incubation experiments (comprising initial, control, and other treatments) were subjected to extraction with 90 % acetone for a duration of 24 h, maintaining a dark and cold environment at −20 °C. This extraction procedure followed the non-acidification method (Welschmeyer, 1994). The resulting extracts were then measured using a Turner Designs Trilogy fluorometer, with calibration performed using a Chl *a* standard from Sigma Aldrich according to the guideline procedure (Parsons et al., 1984).

Second analysis was conducted (without replicate) to assess a set of pigments for the identification of various phytoplankton groups present within the natural community. Volumes of 1 L seawater were filtered from the incubation bottle through Whatman GF/F filters (0.7 μm, 25 mm) via a vacuum filtration system operating at pressures below 10 mmHg. Subsequently, the filters were folded into quarters and preserved at −80 °C in cryotubes until analysis at the Laboratoire d'Océanographie de Villefranche-sur-Mer (Villefranche-sur-Mer, France). Prior to analysis, the filters underwent extraction in a 100 % methanol solution, following the addition of an internal standard addition (vitamin E

acetate, Sigma) and the chromatographic analysis was performed using an Agilent Technologies 1100 series High-Performance Liquid Chromatography system (HPLC) (Ras et al., 2008).

2.7. Identification of phytoplankton groups

Degradation rates, encompassing both grazing and degradation processes, were calculated by aggregating the Phaeopigments, which include Phaeophorbid a and Phaeophytin a (Jeffrey et al., 1997; Wright et al., 2010). These values were then normalized by the total chlorophyll *a* concentration.

$$Degradation\ rate = \frac{Phaeopigments}{Total\ chlorophyll\ a}$$

The HPLC data were subjected to analysis using the Chemtax software (Mackey et al., 1996) with the objective of categorizing them into the principal groups characteristic of the SO. The Chemtax program employs an analysis factor and the steepest descent algorithm to determine the most suitable fit for the data, based on the pigment ratio matrix (supplementary information Table 4).

During the analysis, various phytoplankton groups were categorized into specific types. Haptophytes were differentiated into type 6 (e.g., coccolithophorids) and type 8 (e.g., *Phaeocystis antarctica*) (Zapata et al., 2004). Diatoms were divided into type 1 (e.g., *Thalassiosira* sp. and *Fragilariopsis* sp.) and type 2 (e.g., *Pseudonitzschia* sp.) (Costa et al., 2022; Stauber and Jeffrey, 1988). Prasinophytes were predominantly represented by type 3, primarily composed of the Mamiellales order, as observed in the SO (Scott and Marchant, 2005; Wright et al., 2009). In addition to these classifications, we included ratios for dinoflagellate, cryptophyte, pelagophyte, and chlorophyte groups for both zones. Specifically, the *Synechococcus* group ratios were exclusively incorporated for the PFZ.

2.8. Statistical analysis

An ANOVA test (Fisher, 1992) was initially utilized to assess the significant difference between all the treatments. Subsequently, a complementary Tukey test was employed to conduct pairwise comparisons between the various treatments (Tukey, 1949). It is important to note that the use of statistical tests was suitable when applied to the triplicate fluorometry data, providing adequate statistical power to discern differences. However, for the HPLC data, which lacked replication, these tests were found to be less effective in detecting differences due to limitations in statistical power.

2.9. Estimation of Al input to the Southern Ocean

The estimation of Al input relied on the Fe estimated to the SO amounting to 979 μmol m^{-2} y^{-1} (Henley et al., 2020). This value was then multiplied by the conversion factor 2 to 5, derived from the range ratio of Al and Fe in the Earth's crust (Wedepohl, 1995). The depth of the mixed layer depth (MLD) was assumed to be 60 m, the volume of water 1000 L, and the number of days in a year 365.

$$\text{Input of Al (nmol/L } d^{-1}) = \frac{Input\ of\ Fe\ (nmol\ m^{-2}\ y^{-1}) \times [2\text{–}5]}{Depth\ of\ the\ MLD\ (m) \times volume\ of\ water\ (L) \times number\ of\ days\ in\ the\ year.}$$

3. Results

3.1. Physico-chemical conditions

The measured in situ conditions are depicted in Table 1. Notably, the experiments conducted within the PFZ and the MIZ were at stations occupied at nearly identical geographical coordinates, facilitating a temporal comparison at each site. The daily irradiation duration for the experiments closely followed the prevailing conditions at the time of sampling, showing slight deviations of a few hours.

3.2. Nutrient concentrations

The findings of this study, as summarized in Table 2, indicated that in the PFZ, NO_3 concentrations did not exhibit significant changes over the course of time between October (~24.6 μmol/L) and November (~21.6 μmol/L), nor in the MIZ, where concentrations were approximately ~28.7 μmol/L and ~ 27.3 μmol/L for the respective months. PO_4 concentrations remained within a consistent range across both zones and between the two months, ranging from ~1.50 to 1.92 μmol/L. However, SiO_4 concentrations displayed a notable zonal disparity, with lower concentrations observed in the PFZ (~7.35 μmol/L in October and ~ 5.98 μmol/L in November) and higher concentrations in the MIZ (~43.8 μmol/L in October and ~ 40.2 μmol/L in November).

Dissolved concentrations of trace metals in seawater (Table 2) exhibited an average lower magnitude in the PFZ when compared to the MIZ. Specifically, concentration factors were approximately ~2.6, ~1.7, ~1.9, ~5.0, and ~ 1.2 times greater in the MIZ for Fe, Mn, Cu, Zn, and Co, respectively. The higher concentrations of trace elements and nutrients in the MIZ is the result of deep water upwelling associated with circumpolar deep water, that undergoes south of the Antarctic Polar fronts (Carter et al., 2008).

3.3. Total concentration of chlorophyll a by fluorometry

The results revealed distinct patterns in Chl *a* concentration at the time of sampling. During October, Chl *a* concentrations measured in the control samples of the incubations were notably low, measuring 0.42 μg/L at station 1 and 0.33 μg/L at station 2 (Table 2). These concentrations indicated a state of low productivity (<0.7 μg/L, Bathmann et al., 1997; Fitch and Moore, 2007). In contrast, sampling conducted during November unveiled higher phytoplankton productivity, with Chl *a* concentrations reaching 1.06 μg/L at station 3 and 0.84 μg/L at station 4 (Fig. 2). These concentrations were consistent with phytoplankton bloom conditions in the SO (> 0.7 μg/L, Bathmann et al., 1997; Fitch and Moore, 2007). These observations were further substantiated by satellite images (weekly average) and CTD measurements, confirming the existence of a bloom state (supplementary information, Figs. 1 and 2). Notably, station 3 was sampled at the end of a bloom that likely originated from the sea ice. Within the PFZ, a bloom was in the nascent stages of formation at the time of sampling station 4 (supplementary information, Fig. 2).

After 24 h, significant alterations in Chl *a* concentrations were observed as a result of the metal treatments. The ANOVA test revealed a notable overall difference between treatments, with *p*-values <0.05 for all experiments (experiment 1: 3.55×10^{-7}, experiment 2: 4.79×10^{-7}, experiment 3: 7.01×10^{-7}, and experiment 4: 1.02×10^{-8}) (supplementary information, Table 8). A more detailed analysis, employing the Tukey test for pairwise comparisons between treatments, was conducted to assess significant differences. The outcomes indicated that there were no significant differences between the initial conditions and the control for the first three experiments. However, in experiment 4, a significant difference was noted, characterized by an increase in Chl *a* concentration from 0.84 to 1.16 ± 0.09 μg/L (± 2σ, $n = 3$; Fig. 2).

In experiment 1, the statistical test highlighted significant differences between the Al treatment and the other treatments, as well as between the Fe-Al and Fe-Co treatments in comparison to the control. Specifically, the data demonstrated a substantial reduction in biomass with the addition of Al, resulting in a concentration of 0.08 ± 0.007 μg/L (± 2σ, n = 3). Experiment 2 showed significant differences between the metal spike treatments, indicative of decreased biomass. The most substantial reduction in biomass was also observed with the addition of Al, resulting in a biomass of 0.04 ± 0.004 μg/L (± 2σ, $n = 3$). In experiment 3, the Fe-Al and Fe-Co treatments (0.41 ± 0.02, 0.56 ± 0.01 μg/L, n = 3, respectively) exhibited no significant differences between them.

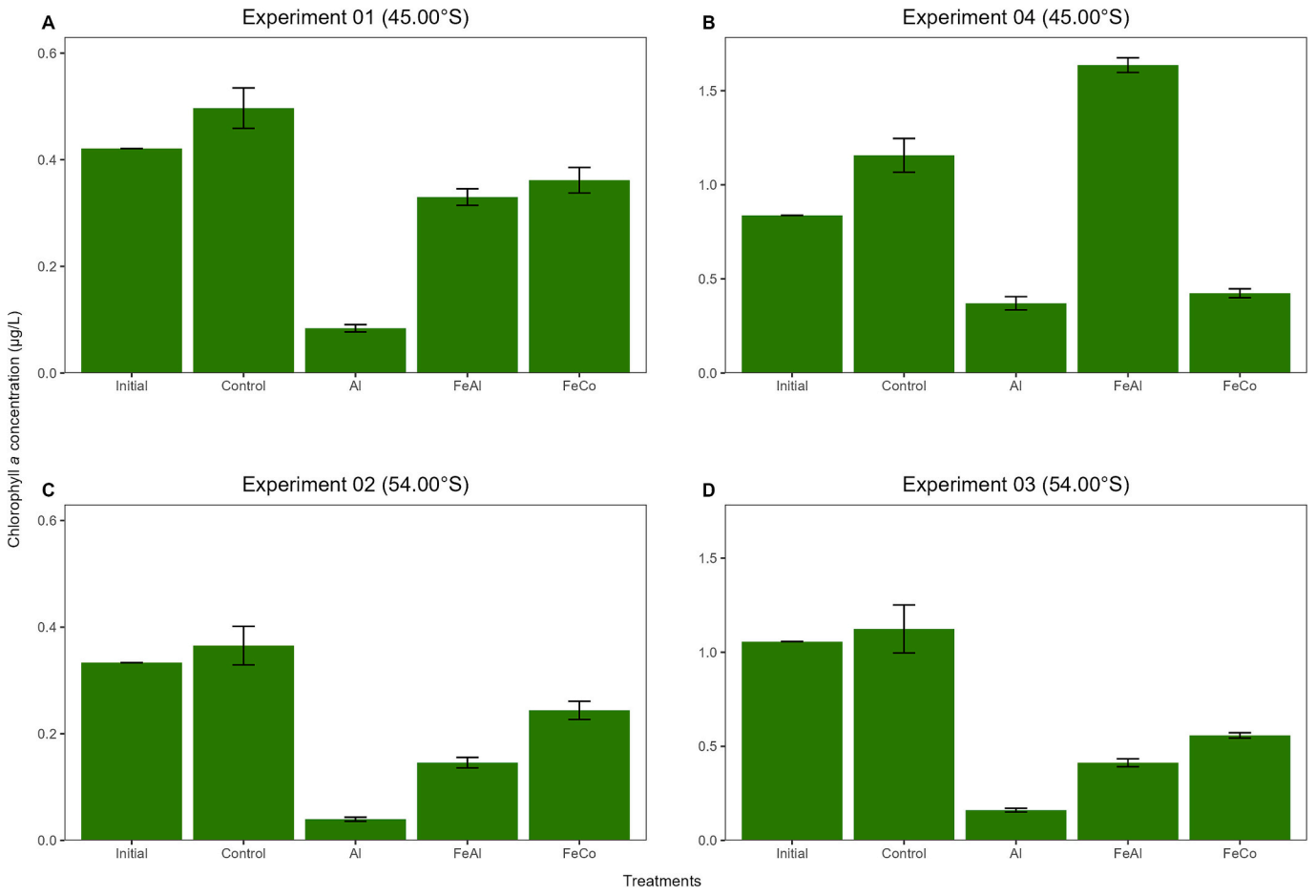

Fig. 2. Total chlorophyll *a* concentration measured by fluorometry in the 4 experiments under the different treatment conditions; Initial represents the Chl *a* concentration measured at the time of seawater sampling, control indicates seawater without any addition of metals after 24 h, Al to the addition of aluminium, Fe-Al to the addition of iron and aluminium, and Fe-Co to the addition of iron and cobalt. The Chl *a* measurements under initial conditions were not replicated, while measurements for the other treatments were conducted in triplicate.

However, both treatments displayed decreased biomass compared to the initial conditions and the control. As observed in earlier experiments, the Al treatment stood out with significant differences from all other tests, leading to the most substantial biomass reduction of 0.16 ± 0.01 µg/L ($n = 3$). In experiment 4, concentrations remained close between the initial conditions and the control (0.84, 1.16 ± 0.09 µg/L, $n = 3$, respectively). Notably, in contrast to the other experiments, the Fe-Al treatment demonstrated a significant increase in biomass, yielding a concentration of 1.64 ± 0.04 µg/L (n = 3). All treatments exhibited significant differences, except for the similarity observed between the Al and Fe-Co treatments, both resulting in the greatest reductions in concentrations (0.37 ± 0.04, 0.42 ± 0.02 µg/L, $n = 3$, respectively).

3.4. Photophysiological response

FRR fluorescence measurements of F_v/F_m and σ_{PSII} within the natural phytoplankton community provide valuable insights into the combined taxonomic and photo-physiological characteristics of phytoplankton cells (Suggett et al., 2009). Under initial conditions (Fig. 3), F_v/F_m values exhibited similarity between experiment 1 and 2, both measuring ~0.42 ± 8.0 × 10^5 ($n = 2$). Likewise, experiment 3 and 4 also displayed analogous F_v/F_m values, both hovering at ~0.33 ± 0.01 (n = 2). The σ_{PSII} values also exhibited consistency, with similar values recorded at 1.82 ± 0.2 nm^2 (n = 2) for experiments 1 and 2, and at 2.12 ± 0.01 nm^2 (n = 2) for experiments 3 and 4.

The ANOVA test unveiled notable overall differences in F_v/F_m measurements across experiments 1, 2, and 4, while these differences were absent in experiment 3 (p-values <0.05; experiment 1: 1.71 × 10^{-11}, experiment 2: 7.92 × 10^{-4}, experiment 3: 7.84 × 10^{-2}, experiment 4: 3.08 × 10^{-3}). In experiment 1, the test discerned significant distinctions among all treatments, except when comparing the initial conditions with the Fe-Co treatment. Generally, all treatments remained close to the values under initial conditions. However, the Al treatment stood out, displaying a significant decrease to 0.17 ± 0.05 (n = 3) (Fig. 3). In experiment 2, significant differences were noted exclusively between the Al treatment and the other treatments. Similar to the previous experiment, the Al treatment exhibited a decrease in F_v/F_m, characterized by a higher standard deviation of 0.10 ± 0.22, (n = 3). Experiments 3 and 4, in contrast to prior experiments, yielded different outcomes, with no significant differences observed between treatments, except in the case of the control and Fe-Al treatments. In both experiments, all treatments closely mirrored the initial conditions.

The ANOVA test applied to σ_{PSII} values demonstrated no significant difference in experiment 1 but revealed significant differences in the other experiments (p-values <0.05; experiment 1: 3.96 × 10^{-1}, experiment 2: 8.33 × 10^{-4}, experiment 3: 5.68 × 10^{-3}, experiment 4: 4.47 × 10^{-3}). In experiment 1, statistical analysis indicated no significant difference among the various treatments, despite a notably higher value of 3.48 ± 3.71 nm^2 (n = 3) observed in the Al treatment, accompanied by substantial variability. In the second experiment, treatment responses exhibited similar trends. In this case, σ_{PSII} also demonstrated an increase, accompanied by notable variability, measuring 4.50 ± 2.23 nm^2 (n = 3). Experiment 3 yielded results consistent with those of experiment 2, with similar pattern differences among treatments. Once again, the Al

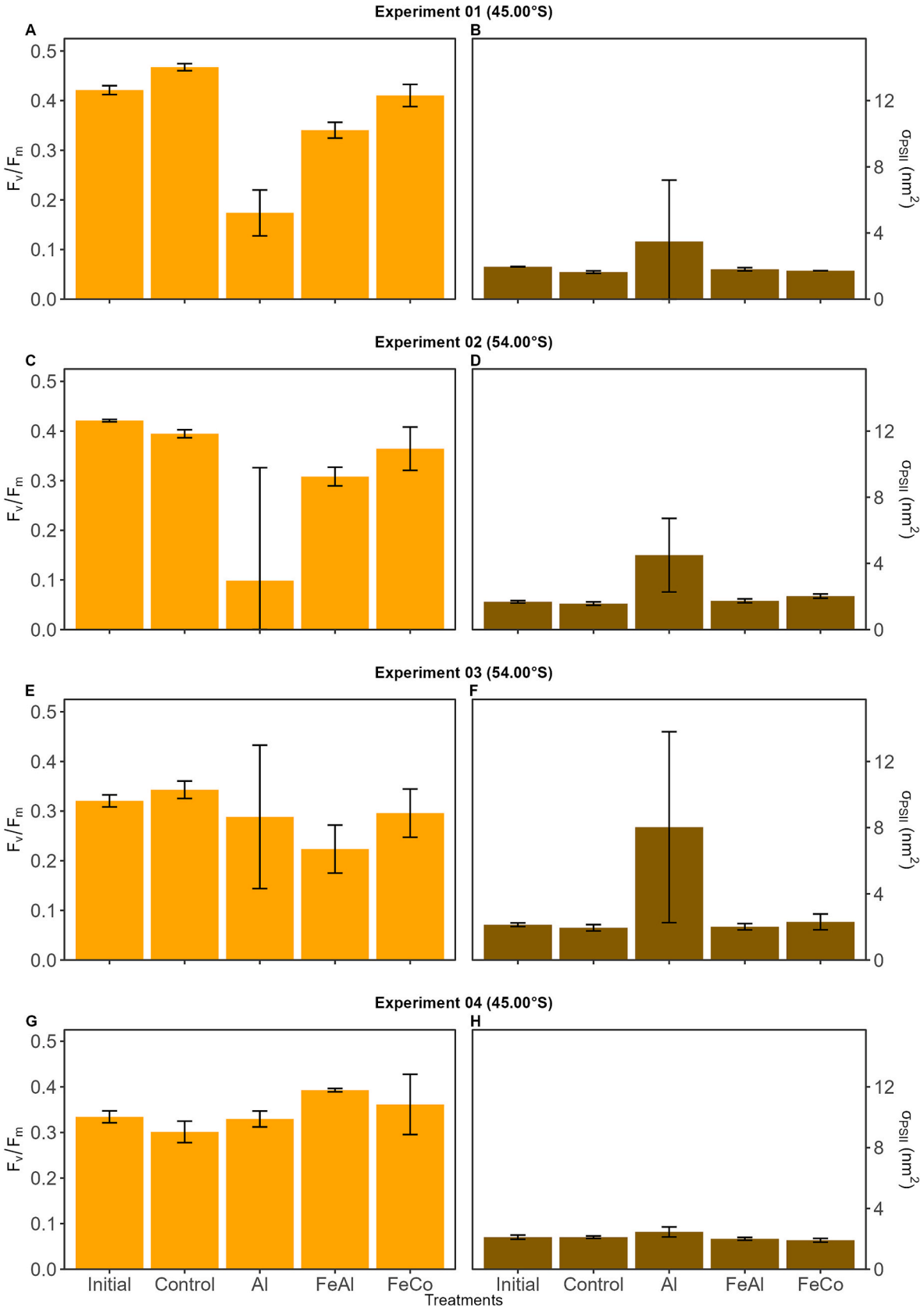

Fig. 3. The mean F_v/F_m (n = 3) and mean σ_{PSII} (nm^2) from the initial, the control, Al treatments, Fe-Al treatments, and Fe-Co treatments for experiment 1, 2, 3 and 4. Values with error bars indicating standard deviations among triplicates.

treatment displayed a similar pattern, featuring an increase in σ_{PSII} accompanied by high variability, measuring 8.02 ± 5.77 nm^2 (n = 3). Similarly, statistical tests conducted on experiment 4 identified differences exclusively between the Al treatment and the control, Fe-Al, and Fe-Co treatments. Unlike the other experiments, the increase in σ_{PSII} was less pronounced in this case, characterized by lower variability at 2.46 ± 0.33 nm^2.

3.5. Distribution of phytoplankton groups

Phytoplankton size classes can exhibit variations in their response to antagonistic or synergistic multi-environmental effects, but more specifically these differences can be visible at the scale of the key groups. Employing Chemtax analysis on HPLC data allowed for the segregation of the natural phytoplankton community into these key groups. Under control conditions (Fig. 4), experiment 1 in the PFZ was predominantly characterized by biomass associated with picophytoplankton, notably *Synechococcus* (0.12 µg/L, 34 %). Nanophytoplankton, mainly comprising prasinophytes (0.07 µg/L, 24 %) and cryptophytes (0.06 µg/L, 19 %), also contributed significantly to the biomass. In contrast, experiment 4, also in the PFZ, showcased dominance by microphytoplankton, particularly diatoms 1 (0.17 µg/L, 29 %) and diatoms 2 (0.11 µg/L, 19 %), alongside a substantial proportion of nanophytoplankton, primarily represented by prasinophytes (0.09 µg/L, 16 %). Both experiments conducted in the MIZ were characterized by a prevalence of microphytoplankton, specifically diatoms 1 (16 % of the total in both experiments 2 and 3) and diatoms 2 (9 % and 38 % in experiment 1 and 3, respectively). Nanophytoplankton, with prasinophytes being a dominant component, was also prominent, with concentrations reaching 0.09 µg/L (53 %) in experiment 2 and 0.10 µg/L (25 %) in experiment 3, mirroring the trends observed in the PFZ.

In the first three experiments, akin to the observations from fluorometry pigment results, a notable reduction in Chl *a* concentration was observed in the Al treatments. This reduction was caused by a loss of biomass across all phytoplankton groups. Notably, the phytoplankton assemblage exhibited no substantial alterations between the control and the Fe-Al and Fe-Co treatments. Specifically, in the Fe-Al treatment, diatom 1 increased from 0 % to 28 % compared to the control. In experiment 4, where the Al-influenced Chl *a* decline was least, no significant change in the phytoplankton assemblage was found, apart for an increase in prasinophytes, which rose from 16 % to 39 % of the natural population.

3.6. Assessment of phytoplankton mortalities

To monitor the phytoplankton mortality, we calculated the phaeopigments/Chl *a* ratio (Fig. 5). The ratios displayed a consistent pattern in the first three experiments, with all treatments exhibiting very low ratios close to 0, except for the Al treatment, which indicated significant cell degradation with ratios of 18.7, 6.0, and 7.4 in experiments 1, 2, and 3,

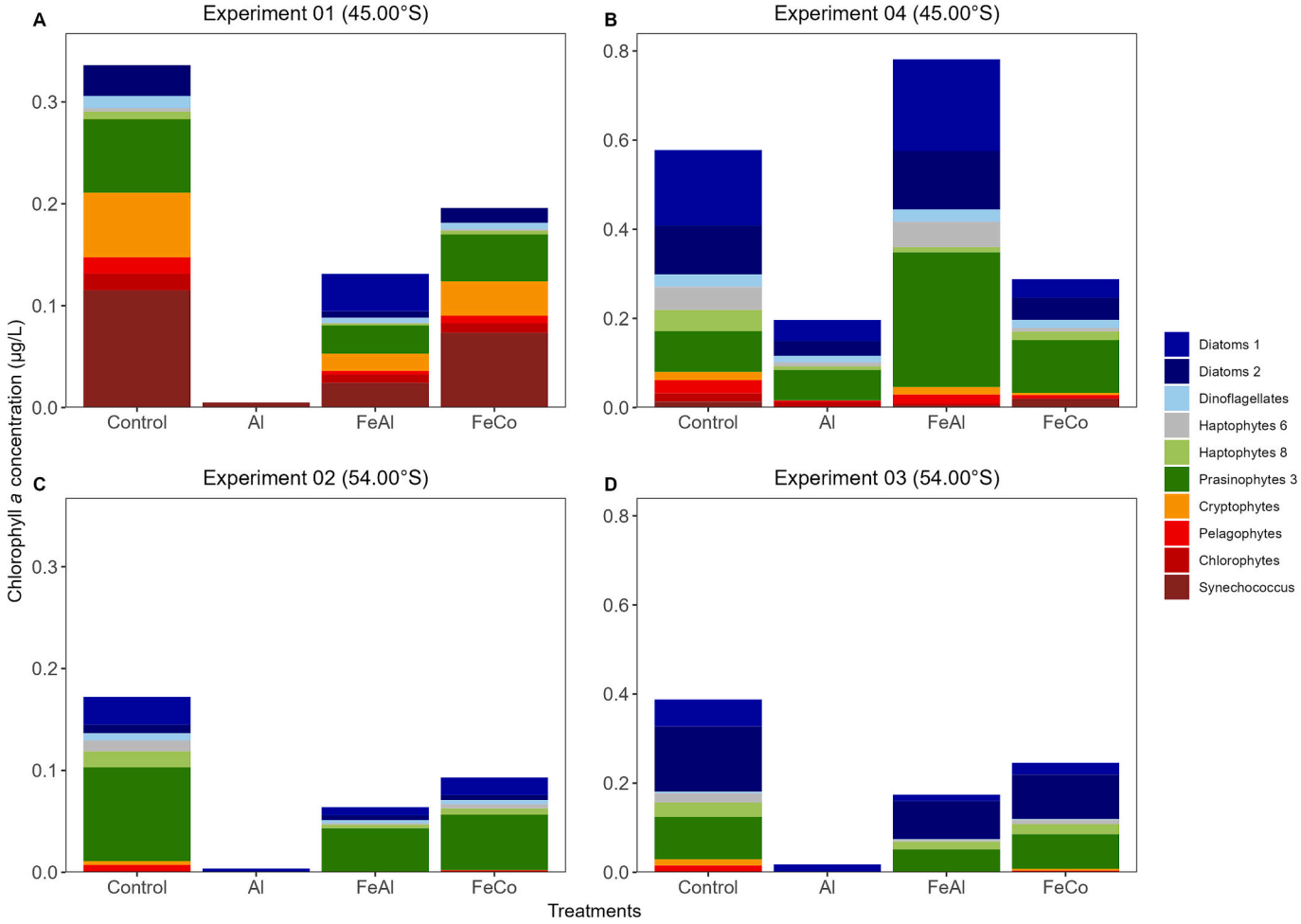

Fig. 4. Chlorophyll *a* concentration (µg/L) of the phytoplankton groups, Chlorophytes (darkblue), Cryptophytes (blue), Diatoms 1 (lightblue), Diatoms 2 (grey), Dinoflagellates (green), Haptophytes 6 (darkgreen), Haptophytes 8 (orange), Pelagophytes (lightred), Prasinophytes 3 (red), Synechococcus (darkred) under the different treatments (Control, Al, FeAl, and FeCo) using Chemtax analyses. Percentage distribution between the different phytoplankton groups is provided in the supplementary information (Fig. 5). (For interpretation of the references to color in this figure legend, the reader is referred to the web version of this article.)

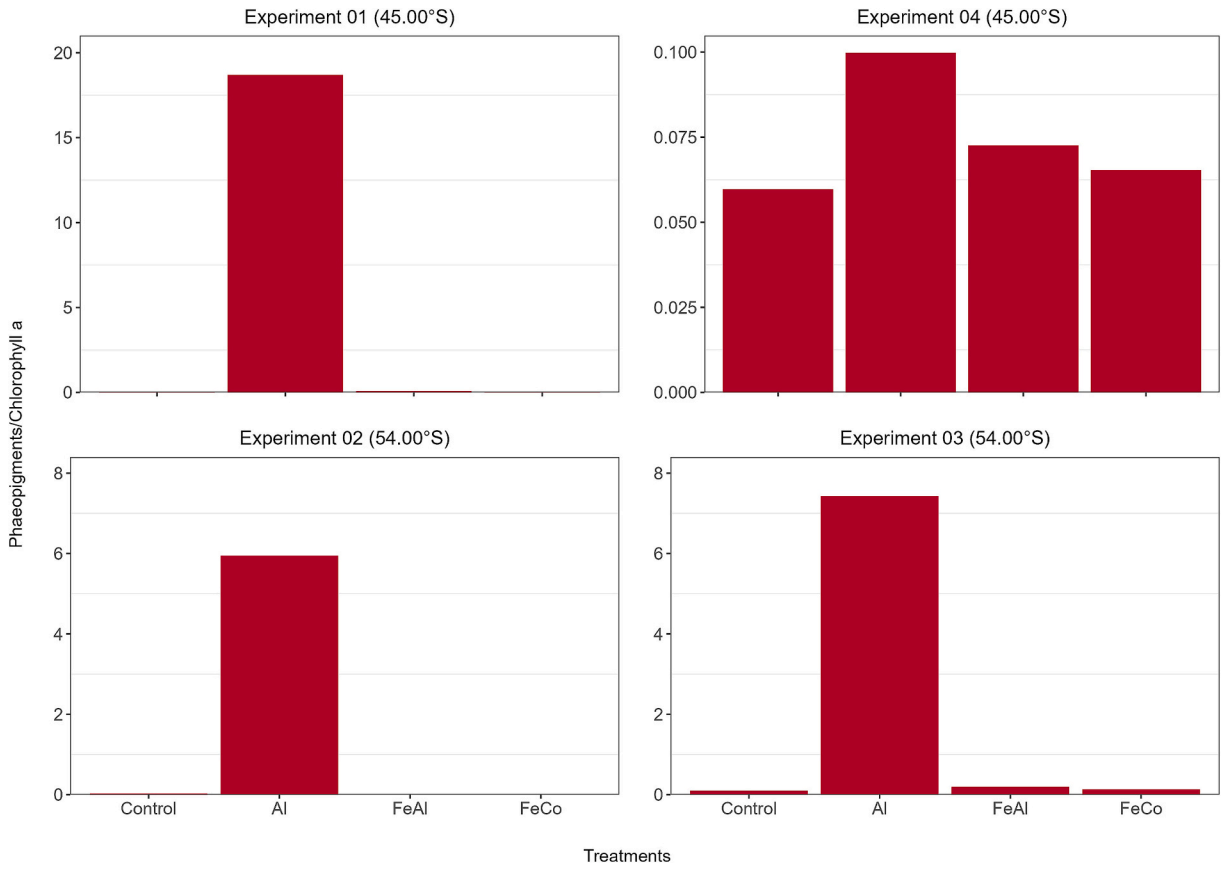

Fig. 5. Phaeopigments/total Chl *a* ratio based on HPLC measurements in the four experiments under the different treatments (Control, Al, FeAl, FeCo). A high ratio indicates phytoplankton cell degradation (Jeffrey et al., 1997). The y-axis varies between graphs.

respectively. Experiment 4, on the other hand, demonstrated a different trend, with lower ratios consistently below 0.1. In this case, all treatments had values centered around 0.07, except for the Al treatment, which recorded a slightly higher ratio of 0.10.

4. Discussion

4.1. Initial conditions

The results indicated consistent initial biogeochemical conditions typical of spring in both zones. Temperature exhibited significant differences between these two distinct biogeochemical zones, aligning with their well-established temperature ranges (Deacon, 1982; Henley et al., 2020; Orsi et al., 1995; Park et al., 1993). However, there were no substantial variations in water temperature at 25 m depth between the months of October and November. In the PFZ, temperatures ranged from 5.3 °C (October) to 5.8 °C (November), while in the MIZ, temperatures ranged from −0.4 °C (October) to −0.2 °C (November). Salinity levels remained relatively stable across both zones and over the observed time frame, with values ranging from 33.94 to 34.18, suggesting the occurrence of Antarctic surface water mass (salinity: 34.04 ± 0.25; Samanta et al., 2023) in the MIZ and in the PFZ. PAR values remained consistent at 129 μmol m^{-2} s^{-1} in the incubator, representing an average light exposure for phytoplankton cells during daylight hours (Biggs et al., 2022). Macronutrient and micronutrient concentrations remain within the ranges of previously published values (Le Moigne et al., 2013; Viljoen et al., 2019). The low concentrations of micronutrients, particularly Fe (Klunder et al., 2011; Martin, 1990), coupled with light limitation (Biggs et al., 2022; Viljoen et al., 2018), may account for the reduced phytoplankton productivity observed in experiments 1 and 2. Nutrient-limited communities exhibited in general a fluorescence signal reflecting a physiological response instead of the taxonomic influence (Suggett et al., 2009). The relatively low F_v/F_m values aligned with previous observations in the SO (Singh et al., 2022; Viljoen et al., 2018), indicating environmental stress (Kolber and Falkowski, 1993) resulting from nutrient and light limitation. In contrast, in experiment 3, representative the end of a bloom, and in experiment 4, marking the beginning of a bloom, the F_v/F_m ratio was lower compared to the other two experiments. This observation may correspond to previous findings where a decrease in F_v/F_m coincides with an increase in cell size during the transition from a cyanobacteria-dominant community to a diatom-dominant one when Fe becomes depleted in the water (Sosik and Olson, 2002).

More specifically, in the PFZ, the low Si values indicated Si limitation (Brzezinski, 1985; Nelson et al., 2001; Sedwick et al., 2002), which accounted for the limited diatom presence, particularly evident in experiment 1. Conversely, the other macronutrients (nitrate and phosphate) were sufficiently abundant to support unrestricted phytoplankton growth (Westwood et al., 2010). Within the MIZ, all macronutrients were found in sufficient concentrations, consistent with regular observations in this zone (Hiscock et al., 2003). The high presence of diatoms in experiments 2 and 3, as commonly observed south of the APF (Gibberd et al., 2013), can be attributed to the elevated concentrations of Si in this region. It is worth noting that F_v/F_m values characteristic of a mixed phytoplankton community were challenging to discern (Suggett et al., 2004). In this case, the observed low values did not align with those typically associated with diatoms (Koblížek et al., 2001; Yentsch et al., 2004).

The results indicated a lower presence of haptophytes 6 compared to prior studies, which have reported significant occurrences of coccolithophores along the great calcite belt located in the PFZ (Balch et al., 2010). This variation can be attributed to the seasonal differences in

sampling, as most previous studies were conducted during the summer (Balch et al., 2019; Boeckel and Baumann, 2008; Patil et al., 2017; Winter et al., 2014). Coccolithophores are known to thrive in waters with temperatures above 8 °C (Findlay and Giraudeau, 2000; Mohan et al., 2008). However, during the course of these experiments, the water temperatures remained consistently below 6 °C in the study area. In the MIZ, the presence of haptophyte 8 was also relatively sparse, despite the literature often reporting blooms of *Phaeocystis antarctica* near the ice shelf (Arrigo et al., 2010). Once again, this difference can be attributed to the timing of these observations, as such blooms have typically been documented during the austral summer.

A notable finding that has been infrequently observed in previous studies is the significant presence of prasinophytes, ranking as the second most abundant phytoplankton group in all experiments. Although some studies have previously reported the robust presence of prasinophytes in the SO, positioning them as the third most abundant group (Viljoen et al., 2018; Wright et al., 2010).

Cyanobacteria were predominantly prevalent in experiment 1, located north of the APF. This distribution aligned with their preference for warmer waters, consistent with prior observations (Viljoen et al., 2018). The F_v/F_m values in this area tended to mirror the dominance of cyanobacteria, in line with previous research (<0.4; Campbell et al., 1998; Koblížek et al., 2001), as cyanobacteria typically exhibit a lower surface-to-volume ratio compared to diatoms.

4.2. Toxicity of aluminium

4.2.1. Effect of toxicity

All treatments exhibited no increase in biomass following the addition of micronutrients, except for experiment 4 with the FeAl treatment. Moreover, there were no discernible disruptions in the distribution of phytoplankton groups. This outcome suggests that the addition of the Fe and Co metals did not appear to be the primary limiting factor for phytoplankton growth. Instead, as previously demonstrated in this region (Viljoen et al., 2018), the availability of light played a pivotal role. The observed variations in biomass were consistent with photophysiological observations (Ryan-Keogh et al., 2013). Specifically, the absence of an increase in biomass corresponded to the absence of an increase in F_v/F_m under the different treatments. This outcome aligned with previous Fe enrichment experiments conducted in the SO, such as IronEx and SOIREE (Boyd and Abraham, 2001; Kolber et al., 1994), which indicated that an augmentation in F_v/F_m was associated with an increase in phytoplankton biomass.

The principal outcome emphasized by these experiments is the toxicity of Al, which led to a decline in phytoplankton biomass in the first three experiments. Notably, these reductions in biomass did not specifically target a particular phytoplankton group but affected the entire natural community. Furthermore, these decreases in biomass were well correlated with the photophysiological results, as evidenced by a decline in F_v/F_m alongside an increase in σ_{PSII}. In the literature, these two observations have primarily been attributed to a reduction in nutrient availability, which can damage the pool of functional reaction centers (RCIIs) responsible for light harvesting (Greene et al., 1992; Kolber et al., 1988; Parkhill et al., 2001; Vassiliev et al., 1995). However, the novelty of these experiments in the PFZ and MIZ suggests that this decline could also be linked to a toxic impact of Al on phytoplankton cells. In our experiments, the phaeopigment-to-Chl *a* ratio emerged as a particularly robust indicator of phytoplankton cell degradation. Notably, the Al treatments displayed elevated values of this ratio. It is worth emphasizing that this degradation was not ascribed to zooplankton grazing, a common explanation in many studies (Jeffrey et al., 1997; Viljoen et al., 2019). In order to maintain conditions closely mirroring natural environments, we deliberately maintained top-down predation in our experiments. The zooplankton community was the same within each incubation, resulting in a similar predation effect on phytoplankton across all treatments. Had zooplankton been responsible for this degradation, we would have observed consistent ratios across all treatments. Consequently, this ratio also presents itself as a potential proxy for assessing the impact of marine pollution.

Nonetheless, it is essential to note that Al had distinct toxic effects across the experiments. In the first two experiments, the decline in biomass might have been intensified because the microalgae were not in a bloom state, which would have left the phytoplankton cells in a dormant state with minimal cell division, hindering their ability to adapt to environmental stress. The impact was particularly pronounced in experiment 1, with the Al treatment exhibiting a lower standard deviation of Fv/F_m compared to the Al treatments of the other experiments. This difference could be attributed to the higher presence of cyanobacteria, which play a more prominent role in photophysiology due to the smaller cells (Suggett et al., 2009). In experiment 3, the significant reduction in biomass can be attributed to a late bloom phase, during which cell division was notably slowed down, thereby limiting the adaptation to Al toxicity. However, in experiment 4, the decline in biomass was less pronounced compared to the other experiments. This relatively minor reduction could be explained by the phytoplankton cells being in a state of active cell division, characteristic of a bloom initiation. Consequently, the accelerated growth rate facilitated a more rapid acclimatization to environmental factors, as cells rely on cell division to adjust to environmental factor (Marvá et al., 2014).

In summary, the variations observed in these experiments indicate that the toxic impact of Al was not contingent on the specific biogeochemical zone or the composition of the natural community. Instead, it appeared to be closely linked to the growth dynamics of the phytoplankton. Under bloom conditions, cells exhibited a heightened state of cell division, reinforcing their capacity to adapt to environmental fluctuations. Conversely, in non-bloom conditions, cells were more sensitive to changes due to their dormant state.

4.2.2. Toxicity linked to the Al concentration

In this study, Al exhibited a toxic effect even at a low concentration of 1 nM, which is considerably lower than the concentrations that typically trigger toxicity, often above the µmol/L range (Gillmore et al., 2016; Golding et al., 2015). Some prior studies have even reported positive effects on phytoplankton growth following Al addition (Zhou et al., 2024; Zhou et al., 2018b), although a clearly defined biological role has not been established. The growth of phytoplankton is a complex interplay of various environmental parameters, with temperature being a primary driver (Boyd et al., 2016), followed by factors such as light, pH, and the availability of macro- and micro-nutrients, all of which can interact synergistically or antagonistically. The previous studies that observed positive effects of Al could potentially be attributed to spatial and seasonal changes or to inadequate control over one or more of these parameters during the incubation process. This distinction can also be ascribed to studies in coastal environments, where natural communities exhibit greater adaptability to high Al concentrations. The toxic effect of Al at such a low concentration in this study, as compared to what has been reported in existing literature, may be explained by the exceptionally low Al concentrations in the SO, which are among the lowest recorded in the world's oceans (Menzel Barraqueta et al., 2020; Middag et al., 2011). Consequently, phytoplankton cells unaccustomed to such nanomolar concentrations of Al may experience stress when exposed to these levels. However, it is important to acknowledge that the study limitation lies in the relatively short 24-h incubation duration, during which only the photophysiological response is anticipated, and thus, may not fully capture the long-term impact on phytoplankton. It is possible that, over a longer timeframe, phytoplankton cells activate acclimatization processes to counteract this stress. Moreover, the experiments revealed that the addition of both Fe and Al led to a lesser decrease in biomass, suggesting that the toxic effect could be mitigated by the supply of essential nutrients like Fe, crucial for cell growth. Hence, under natural lithogenic input, where Al is one of the dominant elements in the crust composition, the bulk of other nutrients such as Fe,

Mn, Co, Zn, and Cu might alleviate this toxic effect. In these experiments, it appeared that the toxic impact of Al may not be solely contingent on the concentration of Al but could also be influenced by its chemical speciation.

4.2.3. Speciation and toxicity mechanisms of Al

The toxic impact of the chemical speciation of Al could not be comprehensively assessed as not quantified in this study. However, it is crucial to acknowledge that the speciation might indeed play a pivotal role in the Al toxicity. The passage of Al into phytoplankton cells could be hindered by its solubility, which is intricately influenced by pH levels and temperature in seawater (Andrade and Costa Marques, 2012; Liu and Millero, 2002; Millero et al., 2009; Saçan and Balcıoğlu, 2001). The solubility of Al in seawater is notably lower when compared to other matrices (Millero et al., 2009; Savenko and Savenko, 2011). Consequently, disparities in the toxic effects of Al in distinct geographical areas and bloom states could be attributed to variations in Al solubility. For instance, the more pronounced toxic impact observed in experiment 3, as compared to experiment 4, could be ascribed to the colder temperatures and lower pH prevalent in the MIZ in contrast to the PFZ (Table 1), resulting in higher Al solubility (Millero et al., 2009). This increased solubility favoured cellular uptake, subsequently leading to heightened toxicity. While there is currently no concrete evidence to support the complexation of Al with siderophores produced by phytoplankton (Santos, 2008), it remains plausible that Al might form complexes with other organic molecules. This potential complexation process might have been more significant in bloom condition (experiments 3 and 4) and particularly for experiment 4 at the development of the bloom (Lorenzo et al., 2007) due to the heightened production of organic ligands. Such a scenario could result in greater Al assimilation and, consequently, increased toxicity. However, it is important to note that this toxic effect was primarily mitigated by the phytoplankton capacity to acclimatize during periods of enhanced cell division and, to a lesser extent, by the reduction in toxicity when Al was complexed with other chemical species.

The experiments conducted in the PFZ and MIZ challenge the potential beneficial influence of Al on phytoplankton metabolism, particularly the Fe-Al hypothesis proposed (Zhou et al., 2018b). This hypothesis suggests that Al could have played a role in climate dynamics during the oscillation between glacial and interglacial periods. However, it is essential to note that this review was not grounded in data specific to the SO; instead, it was based on experiments conducted in the China Sea. Notably, the SO plays a pivotal role in the global oceanic carbon pump (Takahashi et al., 2012), yet no studies to date have focused on evaluating the effect of Fe-Al in this particular region. The proposed rationale for the purported beneficial impact on phytoplankton suggested that Al could facilitate the utilization of Fe, dissolved organic phosphorus, and nitrogen fixation (Zhou et al., 2018b). Additionally, Al was suggested to form bonds with superoxides, creating Al-superoxide complexes (Zhou et al., 2024, Zhou et al., 2018b) which could potentially catalyze the reduction of Fe(III) to the more bioavailable Fe(II) for phytoplankton. Understanding this mechanism could potentially have far-reaching implications for the Al cycle in the world's oceans (Mackenzie et al., 1978). To the best of our current knowledge, no other mechanisms of Al incorporation have been definitively demonstrated for phytoplankton groups. Observations conducted thus far have not provided conclusive evidence of any differences in the mechanisms employed by different phytoplankton groups to incorporate Al into their cells. Nevertheless, the findings of this study, particularly the observed toxic effects of Al, hint at the possibility that alternative mechanisms for Al assimilation may indeed exist. The findings of this study in the SO stand in contrast to the Fe-Al hypothesis, and the purported biological processes have not yet been definitively substantiated.

In parallel, other studies have revealed more intricate interactions among phytoplankton groups than those observed in the SO experiments, where the toxic effects do appear to be species-specific. For example, in the China Sea, the addition of Al was found to stimulate the growth of diatoms and *Trichodesmium* through nitrogen fixation, while inhibiting the growth of dinoflagellates and *Synechococcus* (Zhou et al., 2018a). Numerous studies (e.g. Foy, 1992; Rahman and Upadhyaya, 2021) have explored the toxic repercussions of Al on terrestrial plants. These investigations have highlighted Al capacity to hinder root cell division and DNA synthesis, but it is important to note that the Al concentrations in these terrestrial studies significantly exceeded those employed in the present experiment. Nevertheless, a few isolated studies have provided valuable insights into the observed toxic effects in marine environments. For instance, Al has been implicated in exerting an inhibitory influence on the physiology of *Crocosphaera watsonii*, resulting in phosphorus deficiency (Liu et al., 2020). Another study illustrated that Al could also cause a reduction in the rate of electron transport in the thylakoid membrane, leading to the production of reactive oxygen species (Xie et al., 2015). Associated detrimental impacts have also been documented, including the disruption of the thylakoid membrane and subsequent membrane loss (Saçan et al., 2007).

Considering all environmental parameters, the evaluation of the toxic impact of Al on phytoplankton in the SO presents notable challenges. These challenges stem from various factors, including the quantity and chemical speciation of the Al source, environmental physico-chemical processes, and the acclimatization and adaptation mechanisms of the natural phytoplankton assemblage. Due to experimental constraints, including the 24-h incubation duration, a limited number of experiments, controlled incubator conditions, and the suite of biogeochemical parameters analyzed, these experiments cannot fully replicate all environmental affecting Al toxicity to phytoplankton in the SO (Domingues et al., 2023; Eichel et al., 2014). However, they provide valuable insight into the potential toxic effects of Al at low concentrations, particularly given the consistency observed across the different experiments.

4.3. The Al cycle in the Southern Ocean

The Al cycle in the SO has received limited attention. To comprehend the potential ramifications of this element on natural phytoplankton communities, as well as on climate and the trophic chain (Deppeler and Davidson, 2017; Hauck et al., 2015; Henley et al., 2020), an estimation of Al inputs was performed. The estimated daily Al input was approximately 0.09–0.22 nmol/L d^{-1}, a natural input lower than the concentration utilized in our experiments. Hence, the relatively low lithogenic Al input in the SO is unlikely to induce toxicity in natural communities. This calculation considered average annual inputs, suggesting that a substantial spontaneous event or coastal sediment inputs, like those reported with concentrations of up to 2–3 nmol/L of Al in the Drake Passage (Hatta et al., 2013) or sea ice inputs (1.3–7.2 nmol/L dAl, 0.4–111 nmol/L particulate Al; Lannuzel et al., 2011), exceeding the Al concentration used in our experiment, might indeed have a toxic impact. Nevertheless, these significant inputs were correlated with a proliferation of phytoplankton, as the influx of micronutrients such as Fe could counterbalance the toxic effects, akin to the observations in the Fe-Al treatment. Notably, a sudden lithogenic surge in the SO generally triggers phytoplankton blooms south of the APF (Tripathy and Jena, 2019). This bloom state, coupled by an upsurge in cell division, fosters acclimatization processes, thereby bolstering defence mechanisms against Al toxicity. However, the toxicity of Al could potentially hinge on its chemical form and, consequently, the nature of a lithogenic source. In contrast to the experimental setup, where identical Al inputs were administered in both biogeochemical zones, the chemical form of Al may vary depending on the source, with Al primarily originating from dust in the PFZ (Tagliabue et al., 2009) and predominantly from ice in the MIZ (Tagliabue et al., 2010). Consequently, the lithogenic Al input may not yield the same level of toxicity in different geographical zones within the SO.

5. Conclusion

- This study represents the first attempt to evaluate the impact of Al toxicity on phytoplankton communities within the PFZ and the MIZ of the Atlantic sector of the SO during spring.
- Even at a low concentration of 1 nmol/L, the triggering of Al toxicity to phytoplankton community was observed within a short span of 24 h.
- Toxicity was more pronounced in non-bloom conditions where cell activity was limited whereas the community adapted better in a bloom state where cells were actively dividing. The potential alleviation of an Al toxic effect through the introduction of micronutrients, such as Fe and Co, was also observed during the incubation experiments.
- The overall Al toxicity effect was non-selective, impacting the entire natural community uniformly, without distinction between specific groups or biogeochemical zones within the SO.
- The results emphasize that current in-situ concentrations of Al and other micronutrients in the seawater are unlikely to exert a deleterious impact on natural phytoplankton communities in the open ocean waters. However, this scenario could change with increased localized input of Al, such as those occurring in coastal environments or under changing climatic conditions that enhance lithogenic inputs via dust deposition or glacial melts.

Author contribution

R,A.N secured the funding and overseeing the entire project. D,C. handled the processing and interpretation of all the data, and produced the article. S,S. provided essential assistance with the incubations conducted on board the ship and was responsible for conducting the measurements of dissolved metals. R-K,T. provided the incubators and assisted in data interpretation. S,A. and S,S. prepared all the incubations on board the ship, conducted the incubations during the oceanographic cruise, and supervised the subsequent data analysis. S,A was involved in the measuring and processing of photophysiology data, while S,S. was responsible for conducting the measurements of the dissolved metals. All authors provided valuable input during the drafting and finalization of the manuscript.

Declaration of competing interest

The authors declare that they have no known competing financial interests or personal relationships that could have appeared to influence the work reported in this paper.

Acknowledgments

This research and D,C. was supported by a grant to R,A.N. from an anonymous charitable trust as part of the Whales and Climate Change program (whalesandclimate.org). S,A. and R-K,T. were supported through the CSIR's Southern Ocean Carbon–Climate Observatory (SOCCO) Programme (http://socco.org.za/) funded by the Department of Science and Innovation (DST/CON 0182/2017) and the CSIR's Parliamentary Grant. The experiments were supported by the crew of the research vessel *S.A. Agulhas II*. HPLC analyses were performed at the Laboratoire d'Océanographie de Villefranche-sur-Mer (Villefranche-sur-Mer, France). The authors would also like to thank Jan-Lukas Menzel Barraqueta for his assistance in preparing the incubations.

Appendix A. Supplementary data

Supplementary data to this article can be found online at https://doi.org/10.1016/j.jembe.2025.152119.

Data availability

Data will be made available on request.

References

Andrade, A., Costa Marques, M.R.D., 2012. Electrolytic treatment of wastewater in the oil industry. In: Gomes, J.S. (Ed.), New Technologies in the Oil and Gas Industry. InTech. https://doi.org/10.5772/50712.

Ardyna, M., Lacour, L., Sergi, S., d'Ovidio, F., Sallée, J.-B., Rembauville, M., Blain, S., Tagliabue, A., Schlitzer, R., Jeandel, C., Arrigo, K.R., Claustre, H., 2019. Hydrothermal vents trigger massive phytoplankton blooms in the Southern Ocean. Nat. Commun. 10, 2451. https://doi.org/10.1038/s41467-019-09973-6.

Armand, L.K., Cornet-Barthaux, V., Mosseri, J., Quéguiner, B., 2008. Late summer diatom biomass and community structure on and around the naturally iron-fertilised Kerguelen plateau in the Southern Ocean. Deep Sea Res. Part II Top. Stud. Oceanogr. 55, 653–676. https://doi.org/10.1016/j.dsr2.2007.12.031.

Arrigo, K.R., Van Dijken, G.L., Bushinsky, S., 2008. Primary production in the Southern Ocean, 1997–2006. J. Geophys. Res. Oceans 113, 2007JC004551. https://doi.org/10.1029/2007JC004551.

Arrigo, K.R., Mills, M.M., Kropuenske, L.R., Van Dijken, G.L., Alderkamp, A.-C., Robinson, D.H., 2010. Photophysiology in two major Southern Ocean phytoplankton taxa: photosynthesis and growth of *Phaeocystis antarctica* and *Fragilariopsis cylindrus* under different irradiance levels. Integr. Comp. Biol. 50, 950–966. https://doi.org/10.1093/icb/icq021.

Balch, W.M., Bowler, B.C., Drapeau, D.T., Poulton, A.J., Holligan, P.M., 2010. Biominerals and the vertical flux of particulate organic carbon from the surface ocean. Geophys. Res. Lett. 37. https://doi.org/10.1029/2010GL044640 n/a-n/a.

Balch, W.M., Bowler, B.C., Drapeau, D.T., Lubelczyk, L.C., Lyczkowski, E., Mitchell, C., Wyeth, A., 2019. Coccolithophore distributions of the north and South Atlantic Ocean. Deep Sea Res. Part Oceanogr. Res. Pap. 151, 103066. https://doi.org/10.1016/j.dsr.2019.06.012.

Bathmann, U.V., Scharek, R., Klaas, C., Dubischar, C.D., Smetacek, V., 1997. Spring development of phytoplankton biomass and composition in major water masses of the Atlantic sector of the Southern Ocean. Deep Sea Res. Part II Top. Stud. Oceanogr. 44, 51–67. https://doi.org/10.1016/S0967-0645(96)00063-X.

Biggs, T.E.G., Rozema, P.D., Evans, C., Timmermans, K.R., Meredith, M.P., Pond, D.W., Brussaard, C.P.D., 2022. Control of Antarctic phytoplankton community composition and standing stock by light availability. Polar Biol. 45, 1635–1653. https://doi.org/10.1007/s00300-022-03094-5.

Bilgrami, K.S., Kumar, S., 1997. Effects of copper, lead and zinc on phytoplankton growth. Biol. Plant. 39, 315–317. https://doi.org/10.1023/A:1000600503710.

Boeckel, B., Baumann, K.-H., 2008. Vertical and lateral variations in coccolithophore community structure across the subtropical frontal zone in the South Atlantic Ocean. Mar. Micropaleontol. 67, 255–273. https://doi.org/10.1016/j.marmicro.2008.01.014.

Botté, A., Zaidi, M., Guery, J., Fichet, D., Leignel, V., 2022. Aluminium in aquatic environments: abundance and ecotoxicological impacts. Aquat. Ecol. 56, 751–773. https://doi.org/10.1007/s10452-021-09936-4.

Boyd, P.W., Abraham, E.R., 2001. Iron-mediated changes in phytoplankton photosynthetic competence during SOIREE. Deep Sea Res. Part II Top. Stud. Oceanogr. 48, 2529–2550. https://doi.org/10.1016/S0967-0645(01)00007-8.

Boyd, P.W., Dillingham, P.W., McGraw, C.M., Armstrong, E.A., Cornwall, C.E., Feng, Y.-Y., Hurd, C.L., Gault-Ringold, M., Roleda, M.Y., Timmins-Schiffman, E., Nunn, B.L., 2016. Physiological responses of a Southern Ocean diatom to complex future ocean conditions. Nat. Clim. Chang. 6, 207–213. https://doi.org/10.1038/nclimate2811.

Browning, T.J., Achterberg, E.P., Engel, A., Mawji, E., 2021. Manganese co-limitation of phytoplankton growth and major nutrient drawdown in the Southern Ocean. Nat. Commun. 12, 884. https://doi.org/10.1038/s41467-021-21122-6.

Brzezinski, M.A., 1985. The Si:C:N Ratio of marine diatoms: interspecific variability and the effect of some environmental variables1. J. Phycol. 21, 347–357. https://doi.org/10.1111/j.0022-3646.1985.00347.x.

Brzezinski, M.A., Dickson, M.-L., Nelson, D.M., Sambrotto, R., 2003. Ratios of Si, C and N uptake by microplankton in the Southern Ocean. Deep Sea Res. Part II Top. Stud. Oceanogr. 50, 619–633. https://doi.org/10.1016/S0967-0645(02)00587-8.

Campbell, D., Hurry, V., Clarke, A.K., Gustafsson, P., Öquist, G., 1998. Chlorophyll fluorescence analysis of cyanobacterial photosynthesis and acclimation. Microbiol. Mol. Biol. Rev. 62, 667–683. https://doi.org/10.1128/MMBR.62.3.667-683.1998.

Carter, L., McCave, I.N., Williams, M.J.M., 2008. Chapter 4 circulation and water masses of the Southern Ocean: a review. In: Developments in Earth and Environmental Sciences. Elsevier, pp. 85–114. https://doi.org/10.1016/S1571-9197(08)00004-9.

Costa, R.R., Mendes, C.R.B., Souza, M.S.D., Tavano, V.M., Secchi, E.R., 2022. Chemotaxonomic characterization of the key genera of diatoms in the northern Antarctic peninsula. An. Acad. Bras. Ciênc. 94, e20210584. https://doi.org/10.1590/0001-3765202220210584.

Cullen, J.J., Davis, R.F., 2003. The blank can make a big difference in oceanographic measurements. Limnol. Oceanogr. Bull. 12, 29–35. https://doi.org/10.1002/lob.200312229.

Cutter, G., Casciotti, K., Croot, P., Geibert, W., Heimbürger, L.-E., Lohan, M., Planquette, H., Van De Flierdt, T., 2017. Sampling and Sample-handling Protocols for GEOTRACES Cruises. Version 3, August 2017. GEOTRACES International Project Office, Toulouse, France. https://doi.org/10.25607/OBP-2.

Deacon, G.E.R., 1982. Physical and biological zonation in the Southern Ocean. Deep Sea Res. Part Oceanogr. Res. Pap. 29, 1–15. https://doi.org/10.1016/0198-0149(82)90058-9.
Deppeler, S.L., Davidson, A.T., 2017. Southern Ocean phytoplankton in a changing climate. Front. Mar. Sci. 4. https://doi.org/10.3389/fmars.2017.00040.
Domingues, R.B., Mosley, B.A., Nogueira, P., Maia, I.B., Barbosa, A.B., 2023. Duration, but not bottle volume, affects phytoplankton community structure and growth rates in microcosm experiments. Water 15, 372. https://doi.org/10.3390/w15020372.
Dubischar, C.D., Bathmann, U.V., 1997. Grazing impact of copepods and salps on phytoplankton in the Atlantic sector of the Southern Ocean. Deep Sea Res. Part II Top. Stud. Oceanogr. 44, 415–433. https://doi.org/10.1016/S0967-0645(96)00064-1.
Ducklow, H., Steinberg, D., Buesseler, K., 2001. Upper Ocean carbon export and the biological pump. Oceanography 14, 50–58. https://doi.org/10.5670/oceanog.2001.06.
Egan, L., 2008. Nitrate and/or Nitrite in Brackish or Seawater. Lachat Instruments, Colorado, USA.
Eichel, K.A., Macrae, M.L., Hall, R.I., Fishback, L., Wolfe, B.B., 2014. Nutrient uptake and short-term responses of phytoplankton and benthic algal communities from a subarctic Pond to experimental nutrient enrichment in microcosms. Arct. Antarct. Alp. Res. 46, 191–205. https://doi.org/10.1657/1938-4246-46.1.191.
Eriksen, R., Trull, T., Davies, D., Jansen, P., Davidson, A., Westwood, K., Van Den Enden, R., 2018. Seasonal succession of phytoplankton community structure from autonomous sampling at the Australian Southern Ocean time series (SOTS) observatory. Mar. Ecol. Prog. Ser. 589, 13–31. https://doi.org/10.3354/meps12420.
Findlay, C.S., Giraudeau, J., 2000. Extant calcareous nannoplankton in the Australian sector of the Southern Ocean (austral summers 1994 and 1995). Mar. Micropaleontol. 40, 417–439. https://doi.org/10.1016/S0377-8398(00)00046-3.
Fisher, R.A., 1992. Statistical methods for research workers. In: Kotz, S., Johnson, N.L. (Eds.), Breakthroughs in Statistics, Springer Series in Statistics. Springer New York, New York, NY, pp. 66–70. https://doi.org/10.1007/978-1-4612-4380-9_6.
Fitch, D.T., Moore, J.K., 2007. Wind speed influence on phytoplankton bloom dynamics in the Southern Ocean marginal ice zone. J. Geophys. Res. 112, C08006. https://doi.org/10.1029/2006JC004061.
Flynn, R.F., Haraguchi, L., McQuaid, J., Burger, J.M., Mutseka Lunga, P., Stirnimann, L., Samanta, S., Roychoudhury, A.N., Fawcett, S.E., 2023. Nanoplankton: the dominant vector for carbon export across the Atlantic Southern Ocean in spring. Sci. Adv. 9, eadi3059. https://doi.org/10.1126/sciadv.adi3059.
Foy, C.D., 1992. Soil chemical factors limiting plant root growth. In: Hatfield, J.L., Stewart, B.A. (Eds.), Limitations to Plant Root Growth, Advances in Soil Science. Springer New York, New York, NY, pp. 97–149. https://doi.org/10.1007/978-1-4612-2894-3_5.
Gensemer, R.W., Playle, R.C., 1999. The bioavailability and toxicity of aluminum in aquatic environments. Crit. Rev. Environ. Sci. Technol. 29, 315–450. https://doi.org/10.1080/10643389991259245.
Gibberd, M.-J., Kean, E., Barlow, R., Thomalla, S., Lucas, M., 2013. Phytoplankton chemotaxonomy in the Atlantic sector of the Southern Ocean during late summer 2009. Deep Sea Res. Part Oceanogr. Res. Pap. 78, 70–78. https://doi.org/10.1016/j.dsr.2013.04.007.
Gillmore, M.L., Golding, L.A., Angel, B.M., Adams, M.S., Jolley, D.F., 2016. Toxicity of dissolved and precipitated aluminium to marine diatoms. Aquat. Toxicol. 174, 82–91. https://doi.org/10.1016/j.aquatox.2016.02.004.
Gitelman, H.J. (Ed.), 1989. Aluminum and Health: A Critical Review. Dekker, New York.
Golding, L.A., Angel, B.M., Batley, G.E., Apte, S.C., Krassoi, R., Doyle, C.J., 2015. Derivation of a water quality guideline for aluminium in marine waters. Environ. Toxicol. Chem. 34, 141–151. https://doi.org/10.1002/etc.2771.
Grasshoff, K., Anderson, L.G., Anderson, L. (Eds.), 1999. Methods of Seawater Analysis, Third, Completely Revised and Extended, Edition. ed. Wiley-VCH, Weinheim.
Greene, R.M., Geider, R.J., Kolber, Z., Falkowski, P.G., 1992. Iron-induced changes in light harvesting and photochemical energy conversion processes in eukaryotic marine algae. Plant Physiol. 100, 565–575. https://doi.org/10.1104/pp.100.2.565.
Hatta, M., Measures, C.I., Selph, K.E., Zhou, M., Hiscock, W.T., 2013. Iron fluxes from the shelf regions near the South Shetland Islands in the Drake Passage during the austral-winter 2006. Deep Sea Res. Part II Top. Stud. Oceanogr. 90, 89–101. https://doi.org/10.1016/j.dsr2.2012.11.003.
Hauck, J., Völker, C., Wolf-Gladrow, D.A., Laufkötter, C., Vogt, M., Aumont, O., Bopp, L., Buitenhuis, E.T., Doney, S.C., Dunne, J., Gruber, N., Hashioka, T., John, J., Quéré, C. L., Lima, I.D., Nakano, H., Séférian, R., Totterdell, I., 2015. On the Southern Ocean CO_2 uptake and the role of the biological carbon pump in the 21st century. Glob. Biogeochem. Cycles 29, 1451–1470. https://doi.org/10.1002/2015GB005140.
Henley, S.F., Cavan, E.L., Fawcett, S.E., Kerr, R., Monteiro, T., Sherrell, R.M., Bowie, A. R., Boyd, P.W., Barnes, D.K.A., Schloss, I.R., Marshall, T., Flynn, R., Smith, S., 2020. Changing biogeochemistry of the Southern Ocean and its ecosystem implications. Front. Mar. Sci. 7, 581. https://doi.org/10.3389/fmars.2020.00581.
Hiscock, M.R., Marra, J., Smith, W.O., Goericke, R., Measures, C., Vink, S., Olson, R.J., Sosik, H.M., Barber, R.T., 2003. Primary productivity and its regulation in the Pacific sector of the Southern Ocean. Deep Sea Res. Part II Top. Stud. Oceanogr. 50, 533–558. https://doi.org/10.1016/S0967-0645(02)00583-0.
Jeffrey, S.W., Mantoura, R.F.C., Wright, S.W., International Council of Scientific Unions, Unesco (Eds.), 1997. Phytoplankton Pigments in Oceanography: Guidelines to Modern Methods, Monographs on Oceanographic Methodology. UNESCO Pub, Paris.
Johnson, S., Audh, R.R., De Jager, W., Matlakala, B., Vichi, M., Womack, A., Rampai, T., 2023. Physical and morphological properties of first-year Antarctic Sea ice in the spring marginal ice zone of the Atlantic-Indian sector. J. Glaciol. 1–14. https://doi.org/10.1017/jog.2023.21.
Kangueehi, K.I., 2021. Southern African Dust Characteristics and Potential Impacts on the Surrounding Oceans (PhD Thesis). Stellenbosch University, Stellenbosch.
Klunder, M.B., Laan, P., Middag, R., De Baar, H.J.W., Van Ooijen, J.C., 2011. Dissolved iron in the Southern Ocean (Atlantic sector). Deep Sea Res. Part II Top. Stud. Oceanogr. 58, 2678–2694. https://doi.org/10.1016/j.dsr2.2010.10.042.
Koblížek, M., Kaftan, D., Nedbal, L., 2001. On the relationship between the non-photochemical quenching of the chlorophyll fluorescence and the photosystem II light harvesting efficiency. A repetitive flash fluorescence induction study. Photosynth. Res. 68, 141–152. https://doi.org/10.1023/A:1011830015167.
Kolber, Z., Falkowski, P.G., 1993. Use of active fluorescence to estimate phytoplankton photosynthesis in situ. Limnol. Oceanogr. 38, 1646–1665. https://doi.org/10.4319/lo.1993.38.8.1646.
Kolber, Z., Zehr, J., Falkowski, P., 1988. Effects of growth irradiance and nitrogen limitation on photosynthetic energy conversion in photosystem II. Plant Physiol. 88, 923–929. https://doi.org/10.1104/pp.88.3.923.
Kolber, Z.S., Barber, R.T., Coale, K.H., Fitzwateri, S.E., Greene, R.M., Johnson, K.S., Lindley, S., Falkowski, P.G., 1994. Iron limitation of phytoplankton photosynthesis in the equatorial Pacific Ocean. Nature 371, 145–149. https://doi.org/10.1038/371145a0.
Koning, E., Gehlen, M., Flank, A.-M., Calas, G., Epping, E., 2007. Rapid post-mortem incorporation of aluminum in diatom frustules: evidence from chemical and structural analyses. Mar. Chem. 106, 208–222. https://doi.org/10.1016/j.marchem.2006.06.009.
Kopczyńska, E.E., Savoye, N., Dehairs, F., Cardinal, D., Elskens, M., 2007. Spring phytoplankton assemblages in the Southern Ocean between Australia and Antarctica. Polar Biol. 31, 77–88. https://doi.org/10.1007/s00300-007-0335-6.
Lannuzel, D., Schoemann, V., De Jong, J., Chou, L., Delille, B., Becquevort, S., Tison, J.-L., 2008. Iron study during a time series in the western Weddell pack ice. Mar. Chem. 108, 85–95. https://doi.org/10.1016/j.marchem.2007.10.006.
Lannuzel, D., Bowie, A.R., Van Der Merwe, P.C., Townsend, A.T., Schoemann, V., 2011. Distribution of dissolved and particulate metals in Antarctic Sea ice. Mar. Chem. 124, 134–146. https://doi.org/10.1016/j.marchem.2011.01.004.
Le Moigne, F.A.C., Boye, M., Masson, A., Corvaisier, R., Grossteffan, E., Guéneugues, A., Pondaven, P., 2013. Description of the biogeochemical features of the subtropical southeastern Atlantic and the Southern Ocean south of South Africa during the austral summer of the international polar year. Biogeosciences 10, 281–295. https://doi.org/10.5194/bg-10-281-2013.
Liu, X., Millero, F.J., 2002. The solubility of iron in seawater. Mar. Chem. 77, 43–54. https://doi.org/10.1016/S0304-4203(01)00074-3.
Liu, Q., Zhou, L., Liu, F., Fortin, C., Tan, Y., Huang, L., Campbell, P.G.C., 2019. Uptake and subcellular distribution of aluminum in a marine diatom. Ecotoxicol. Environ. Saf. 169, 85–92. https://doi.org/10.1016/j.ecoenv.2018.10.095.
Liu, J., Zhou, L., Ke, Z., Li, G., Tan, Y., 2020. Phosphorus deficiency induced by aluminum in a marine nitrogen-fixing cyanobacterium Crocosphaera watsonii WH0003. Chemosphere 246, 125641. https://doi.org/10.1016/j.chemosphere.2019.125641.
Lohan, M.C., Tagliabue, A., 2018. Oceanic micronutrients: trace metals that are essential for marine life. Elements 14, 385–390. https://doi.org/10.2138/gselements.14.6.385.
Lorenzo, J.I., Nieto-Cid, M., Álvarez-Salgado, X.A., Pérez, P., Beiras, R., 2007. Contrasting complexing capacity of dissolved organic matter produced during the onset, development and decay of a simulated bloom of the marine diatom *Skeletonema costatum*. Mar. Chem. 103, 61–75. https://doi.org/10.1016/j.marchem.2006.05.009.
Lourey, M.J., Trull, T.W., 2001. Seasonal nutrient depletion and carbon export in the Subantarctic and polar frontal zones of the Southern Ocean south of Australia. J. Geophys. Res. Oceans 106, 31463–31487. https://doi.org/10.1029/2000JC000287.
Macdonald, T.L., Martin, B.R., 1988. Aluminum ion in biological systems. Trends Biochem. Sci. 13, 15–19. https://doi.org/10.1016/0968-0004(88)90012-6.
Machill, S., Köhler, L., Ueberlein, S., Hedrich, R., Kunaschk, M., Paasch, S., Schulze, R., Brunner, E., 2013. Analytical studies on the incorporation of aluminium in the cell walls of the marine diatom *Stephanopyxis turris*. BioMetals 26, 141–150. https://doi.org/10.1007/s10534-012-9601-3.
Mackenzie, F.T., Stoffyn, M., Wollast, R., 1978. Aluminum in seawater: control by biological activity. Science 199, 680–682. https://doi.org/10.1126/science.199.4329.680.
Mackey, M., Mackey, D., Higgins, H., Wright, S., 1996. CHEMTAX - a program for estimating class abundances from chemical markers:application to HPLC measurements of phytoplankton. Mar. Ecol. Prog. Ser. 144, 265–283. https://doi.org/10.3354/meps144265.
Mahowald, N.M., Baker, A.R., Bergametti, G., Brooks, N., Duce, R.A., Jickells, T.D., Kubilay, N., Prospero, J.M., Tegen, I., 2005. Atmospheric global dust cycle and iron inputs to the ocean: atmospheric iron deposition. Glob. Biogeochem. Cycles 19. https://doi.org/10.1029/2004GB002402.
Martin, J.H., 1990. Glacial-interglacial CO2 change the Iron hypothesis. Paleoceanography 5, 13.
Martin, J.H., Knauer, G.A., 1973. The elemental composition of plankton. Geochim. Cosmochim. Acta 37, 1639–1653. https://doi.org/10.1016/0016-7037(73)90154-3.
Marvá, F., García-Balboa, C., Baselga-Cervera, B., Costas, E., 2014. Rapid adaptation of some phytoplankton species to osmium as a result of spontaneous mutations. Ecotoxicology 23, 213–220. https://doi.org/10.1007/s10646-013-1164-8.
Menzel Barraqueta, J.-L., Samanta, S., Achterberg, E.P., Bowie, A.R., Croot, P., Cloete, R., De Jongh, T., Gelado-Caballero, M.D., Klar, J.K., Middag, R., Loock, J.C., Remenyi, T.A., Wenzel, B., Roychoudhury, A.N., 2020. A first global oceanic

compilation of observational dissolved aluminum data with regional statistical data treatment. Front. Mar. Sci. 7, 468. https://doi.org/10.3389/fmars.2020.00468.
Middag, R., Van Slooten, C., De Baar, H.J.W., Laan, P., 2011. Dissolved aluminium in the Southern Ocean. Deep Sea Res. Part II Top. Stud. Oceanogr. 58, 2647–2660. https://doi.org/10.1016/j.dsr2.2011.03.001.
Miller, R.J., Lenihan, H.S., Muller, E.B., Tseng, N., Hanna, S.K., Keller, A.A., 2010. Impacts of metal oxide nanoparticles on marine phytoplankton. Environ. Sci. Technol. 44, 7329–7334. https://doi.org/10.1021/es100247x.
Millero, F.J., Woosley, R., Ditrolio, B., Waters, J., 2009. Effect of ocean acidification on the speciation of metals in seawater. Oceanography 22, 72–85.
Mitchell, B.G., Brody, E.A., Holm-Hansen, O., McClain, C., Bishop, J., 1991. Light limitation of phytoplankton biomass and macronutrient utilization in the Southern Ocean. Limnol. Oceanogr. 36, 1662–1677. https://doi.org/10.4319/lo.1991.36.8.1662.
Mohan, R., Mergulhao, L.P., Guptha, M.V.S., Rajakumar, A., Thamban, M., AnilKumar, N., Sudhakar, M., Ravindra, R., 2008. Ecology of coccolithophores in the Indian sector of the Southern Ocean. Mar. Micropaleontol. 67, 30–45. https://doi.org/10.1016/j.marmicro.2007.08.005.
Moore, J.K., Abbott, M.R., 2000. Phytoplankton chlorophyll distributions and primary production in the Southern Ocean. J. Geophys. Res. Oceans 105, 28709–28722. https://doi.org/10.1029/1999JC000043.
Moran, S.B., Moore, R.M., 1988. Evidence from mesocosm studies for biological removal of dissolved aluminium from sea water. Nature 335, 706–708. https://doi.org/10.1038/335706a0.
SEAWIFS-ORBVIEW-2 Level 2 Ocean Color Data Version R2018.0, 2018. NASA Ocean Biology Processing Group. https://doi.org/10.5067/ORBVIEW-2/SEAWIFS/L2/OC/2018.
Nelson, D.M., Smith, W., 1991. Sverdrup revisited: critical depths, maximum chlorophyll levels, and the control of Southern Ocean productivity by the irradiance-mixing regime. Limnol. Oceanogr. 36, 1650–1661. https://doi.org/10.4319/lo.1991.36.8.1650.
Nelson, D.M., Brzezinski, M.A., Sigmon, D.E., Franck, V.M., 2001. A seasonal progression of Si limitation in the Pacific sector of the Southern Ocean. Deep Sea Res. Part II Top. Stud. Oceanogr. 48, 3973–3995. https://doi.org/10.1016/S0967-0645(01)00076-5.
Okamura, H., Aoyama, I., 1994. Interactive toxic effect and distribution of heavy metals in phytoplankton. Environ. Toxicol. Water Qual. 9, 7–15. https://doi.org/10.1002/tox.2530090103.
Orsi, A.H., Whitworth, T., Nowlin, W.D., 1995. On the meridional extent and fronts of the Antarctic circumpolar current. Deep Sea Res. Part Oceanogr. Res. Pap. 42, 641–673. https://doi.org/10.1016/0967-0637(95)00021-W.
Park, Y.-H., Gamberoni, L., Charriaud, E., 1993. Frontal structure, water masses, and circulation in the Crozet Basin. J. Geophys. Res. 98, 12361. https://doi.org/10.1029/93JC00938.
Parkhill, J.-P., Maillet, G., Cullen, J.J., 2001. Fluorescence-based maximal quantum yield for PSII as a diagnostic of nutrient stress. J. Phycol. 37, 517–529. https://doi.org/10.1046/j.1529-8817.2001.037004517.x.
Parsons, T.R., Maita, Y., Lalli, C.M., 1984. A Manual of Chemical and Biological Methods for Seawater Analysis, repr. ed. Pergamon Press, Oxford.
Patil, S.M., Mohan, R., Shetye, S.S., Gazi, S., Baumann, K.-H., Jafar, S., 2017. Biogeographic distribution of extant Coccolithophores in the Indian sector of the Southern Ocean. Mar. Micropaleontol. 137, 16–30. https://doi.org/10.1016/j.marmicro.2017.08.002.
Paytan, A., Mackey, K.R.M., Chen, Y., Lima, I.D., Doney, S.C., Mahowald, N., Labiosa, R., Post, A.F., 2009. Toxicity of atmospheric aerosols on marine phytoplankton. Proc. Natl. Acad. Sci. 106, 4601–4605. https://doi.org/10.1073/pnas.0811486106.
Planquette, H., Fones, G.R., Statham, P.J., Morris, P.J., 2009. Origin of iron and aluminium in large particles (>53 μm) in the Crozet region, Southern Ocean. Mar. Chem. 115, 31–42. https://doi.org/10.1016/j.marchem.2009.06.002.
Pollard, R.T., Lucas, M.I., Read, J.F., 2002. Physical controls on biogeochemical zonation in the Southern Ocean. Deep Sea Res. Part II Top. Stud. Oceanogr. 49, 3289–3305. https://doi.org/10.1016/S0967-0645(02)00084-X.
Popp, B.N., Trull, T., Kenig, F., Wakeham, S.G., Rust, T.M., Tilbrook, B., Griffiths, B., Wright, S.W., Marchant, H.J., Bidigare, R.R., Laws, E.A., 1999. Controls on the carbon isotopic composition of southern ocean phytoplankton. Glob. Biogeochem. Cycles 13, 827–843. https://doi.org/10.1029/1999GB900041.
Rahman, R., Upadhyaya, H., 2021. Aluminium toxicity and its tolerance in plant: a review. J. Plant Biol. 64, 101–121. https://doi.org/10.1007/s12374-020-09280-4.
Ras, J., Claustre, H., Uitz, J., 2008. Spatial variability of phytoplankton pigment distributions in the subtropical South Pacific Ocean: comparison between in situ and predicted data. Biogeosciences 5, 353–369. https://doi.org/10.5194/bg-5-353-2008.
Roháček, K., 2002. Chlorophyll fluorescence parameters: the definitions, photosynthetic meaning, and mutual relationships. Photosynthetica 40, 13–29. https://doi.org/10.1023/A:1020125719386.
Rohr, T., Long, M.C., Kavanaugh, M.T., Lindsay, K., Doney, S.C., 2017. Variability in the mechanisms controlling Southern Ocean phytoplankton bloom phenology in an ocean model and satellite observations. Glob. Biogeochem. Cycles 31, 922–940. https://doi.org/10.1002/2016GB005615.
Ross, O., Geider, R., Berdalet, E., Artigas, M., Piera, J., 2011a. Modelling the effect of vertical mixing on bottle incubations for determining in situ phytoplankton dynamics. I. Growth rates. Mar. Ecol. Prog. Ser. 435, 13–31. https://doi.org/10.3354/meps09193.
Ross, O., Geider, R., Piera, J., 2011b. Modelling the effect of vertical mixing on bottle incubations for determining in situ phytoplankton dynamics. II. Primary production. Mar. Ecol. Prog. Ser. 435, 33–45. https://doi.org/10.3354/meps09194.
Ryan-Keogh, T.J., Robinson, C.M., 2021. Phytoplankton Photophysiology utilities: a Python toolbox for the standardization of processing active chlorophyll-a fluorescence data. Front. Mar. Sci. 8, 525414. https://doi.org/10.3389/fmars.2021.525414.
Ryan-Keogh, T.J., Macey, A.I., Nielsdóttir, M.C., Lucas, M.I., Steigenberger, S.S., Stinchcombe, M.C., Achterberg, E.P., Bibby, T.S., Moore, C.M., 2013. Spatial and temporal development of phytoplankton iron stress in relation to bloom dynamics in the high-latitude North Atlantic Ocean. Limnol. Oceanogr. 58, 533–545. https://doi.org/10.4319/lo.2013.58.2.0533.
Saçan, M.T., Balcıoğlu, A., 2001. Bioaccumulation of aluminium in *Dunaliella tertiolecta* in natural seawater: aluminium–metal (Cu, Pb, Se) interactions and influence of pH. Bull. Environ. Contam. Toxicol. 66, 214–221. https://doi.org/10.1007/s0012800227.
Saçan, M.T., Oztay, F., Bolkent, S., 2007. Exposure of *Dunaliella tertiolecta* to lead and aluminum: toxicity and effects on ultrastructure. Biol. Trace Elem. Res. 120, 264–272. https://doi.org/10.1007/s12011-007-8016-4.
Samanta, S., Cloete, R., Loock, J., Rossouw, R., Roychoudhury, A.N., 2021. Determination of trace metal (Mn, Fe, Ni, Cu, Zn, Co, Cd and Pb) concentrations in seawater using single quadrupole ICP-MS: A comparison between offline and online preconcentration setups. Minerals 11, 1289. https://doi.org/10.3390/min11111289.
Samanta, S., Cloete, R., Dey, S.P., Barraqueta, J.-L.M., Loock, J.C., Meynecke, J.-O., De Bie, J., Vichi, M., Roychoudhury, A.N., 2023. Exchange of Pb from Indian to Atlantic Ocean is driven by Agulhas current and atmospheric Pb input from South Africa. Sci. Rep. 13, 5465. https://doi.org/10.1038/s41598-023-32613-5.
Santos, M.A., 2008. Recent developments on 3-hydroxy-4-pyridinones with respect to their clinical applications. Coord. Chem. Rev. 252, 1213–1224. https://doi.org/10.1016/j.ccr.2008.01.033.
Savenko, A.V., Savenko, V.S., 2011. Aluminum hydroxide's solubility and the forms of dissolved aluminum's occurrence in seawater. Oceanology 51, 231–234. https://doi.org/10.1134/S0001437011020147.
Schuback, N., Tortell, P.D., Berman-Frank, I., Campbell, D.A., Ciotti, A., Courtecuisse, E., Erickson, Z.K., Fujiki, T., Halsey, K., Hickman, A.E., Huot, Y., Gorbunov, M.Y., Hughes, D.J., Kolber, Z.S., Moore, C.M., Oxborough, K., Prášil, O., Robinson, C.M., Ryan-Keogh, T.J., Silsbe, G., Simis, S., Suggett, D.J., Thomalla, S., Varkey, D.R., 2021. Single-turnover variable chlorophyll fluorescence as a tool for assessing phytoplankton photosynthesis and primary productivity: opportunities, caveats and recommendations. Front. Mar. Sci. 8, 690607. https://doi.org/10.3389/fmars.2021.690607.
Scott, F.J., Marchant, H.J. (Eds.), 2005. Antarctic Marine Protists. Australian Biological Resources Study and Australian Antarctic Division, Canberra.
Sedwick, P.N., Blain, S., Quéguiner, B., Griffiths, F.B., Fiala, M., Bucciarelli, E., Denis, M., 2002. Resource limitation of phytoplankton growth in the Crozet Basin, Subantarctic Southern Ocean. Deep Sea Res. Part II Top. Stud. Oceanogr. 49, 3327–3349. https://doi.org/10.1016/S0967-0645(02)00086-3.
Shramik, P., Rahul, M., Suhas, S., Sahina, G., 2013. Phytoplankton abundance and community structure in the Antarctic polar frontal region during austral summer of 2009. Chin. J. Oceanol. Limnol. 31, 21–30. https://doi.org/10.1007/s00343-013-1309-x.
Singh, A., Thomalla, S.J., Fietz, S., Ryan-Keogh, T.J., 2022. Spatial and temporal variability of phytoplankton photophysiology in the Atlantic Southern Ocean. Front. Mar. Sci. 9, 912856. https://doi.org/10.3389/fmars.2022.912856.
Smetacek, V., Assmy, P., Henjes, J., 2004. The role of grazing in structuring Southern Ocean pelagic ecosystems and biogeochemical cycles. Antarct. Sci. 16, 541–558. https://doi.org/10.1017/S0954102004002317.
Smith, W.O., Keene, N.K., Comiso, J.C., 1988. Interannual variability in estimated primary productivity of the Antarctic marginal ice zone. In: Sahrhage, D. (Ed.), Antarctic Ocean and Resources Variability. Springer Berlin Heidelberg, Berlin, Heidelberg, pp. 131–139. https://doi.org/10.1007/978-3-642-73724-4_10.
Sokolov, S., Rintoul, S.R., 2007. On the relationship between fronts of the Antarctic circumpolar current and surface chlorophyll concentrations in the Southern Ocean. J. Geophys. Res. Oceans 112, 2006JC004072. https://doi.org/10.1029/2006JC004072.
Sosik, H.M., Olson, R.J., 2002. Phytoplankton and iron limitation of photosynthetic efficiency in the Southern Ocean during late summer. Deep Sea Res. Part Oceanogr. Res. Pap. 49, 1195–1216. https://doi.org/10.1016/S0967-0637(02)00015-8.
Spreen, G., Kaleschke, L., Heygster, G., 2008. Sea ice remote sensing using AMSR-E 89-GHz channels. J. Geophys. Res. 113, C02S03. https://doi.org/10.1029/2005JC003384.
Stauber, J.L., Jeffrey, S.W., 1988. Photosynthetic pigments in fifty-one species of marine diatoms. J. Phycol. 24, 158–172. https://doi.org/10.1111/j.1529-8817.1988.tb04230.x.
Suggett, D., Kraay, G., Holligan, P., Davey, M., Aiken, J., Geider, R., 2001. Assessment of photosynthesis in a spring cyanobacterial bloom by use of a fast repetition rate fluorometer. Limnol. Oceanogr. 46, 802–810. https://doi.org/10.4319/lo.2001.46.4.0802.
Suggett, D.J., MacIntyre, H.L., Geider, R.J., 2004. Evaluation of biophysical and optical determinations of light absorption by photosystem II in phytoplankton: evaluation of light absorption by PSII. Limnol. Oceanogr. Methods 2, 316–332. https://doi.org/10.4319/lom.2004.2.316.
Suggett, D., Moore, C., Hickman, A., Geider, R., 2009. Interpretation of fast repetition rate (FRR) fluorescence: signatures of phytoplankton community structure versus physiological state. Mar. Ecol. Prog. Ser. 376, 1–19. https://doi.org/10.3354/meps07830.

Tagliabue, A., Bopp, L., Aumont, O., 2009. Evaluating the importance of atmospheric and sedimentary iron sources to Southern Ocean biogeochemistry. Geophys. Res. Lett. 36, L13601. https://doi.org/10.1029/2009GL038914.

Tagliabue, A., Bopp, L., Dutay, J.-C., Bowie, A.R., Chever, F., Jean-Baptiste, P., Bucciarelli, E., Lannuzel, D., Remenyi, T., Sarthou, G., Aumont, O., Gehlen, M., Jeandel, C., 2010. Hydrothermal contribution to the oceanic dissolved iron inventory. Nat. Geosci. 3, 252–256. https://doi.org/10.1038/ngeo818.

Tagliabue, A., Hawco, N.J., Bundy, R.M., Landing, W.M., Milne, A., Morton, P.L., Saito, M.A., 2018. The role of external inputs and internal cycling in shaping the Global Ocean cobalt distribution: insights from the first cobalt biogeochemical model. Glob. Biogeochem. Cycles 32, 594–616. https://doi.org/10.1002/2017GB005830.

Takahashi, T., Sweeney, C., Hales, B., Chipman, D., Newberger, T., Goddard, J., Iannuzzi, R., Sutherland, S., 2012. The changing carbon cycle in the Southern Ocean. Oceanography 25, 26–37. https://doi.org/10.5670/oceanog.2012.71.

Thomalla, S.J., Fauchereau, N., Swart, S., Monteiro, P.M.S., 2011. Regional scale characteristics of the seasonal cycle of chlorophyll in the Southern Ocean. Biogeosciences 8, 2849–2866. https://doi.org/10.5194/bg-8-2849-2011.

Thomalla, S.J., Nicholson, S.-A., Ryan-Keogh, T.J., Smith, M.E., 2023. Widespread changes in Southern Ocean phytoplankton blooms linked to climate drivers. Nat. Clim. Chang. 13, 975–984. https://doi.org/10.1038/s41558-023-01768-4.

Tripathy, S.C., Jena, B., 2019. Iron-stimulated phytoplankton blooms in the Southern Ocean: a brief review. Remote Sens. Earth Syst. Sci. 2, 64–77. https://doi.org/10.1007/s41976-019-00012-y.

Tukey, J.W., 1949. Comparing individual means in the analysis of variance. Biometrics 5, 99. https://doi.org/10.2307/3001913.

Van Dam, J.W., Trenfield, M.A., Streten, C., Harford, A.J., Parry, D., Van Dam, R.A., 2018. Water quality guideline values for aluminium, gallium and molybdenum in marine environments. Environ. Sci. Pollut. Res. 25, 26592–26602. https://doi.org/10.1007/s11356-018-2702-y.

Vassiliev, I.R., Kolber, Z., Wyman, K.D., Mauzerall, D., Shukla, V.K., Falkowski, P.G., 1995. Effects of Iron limitation on photosystem II composition and light utilization in *Dunaliella tertiolecta*. Plant Physiol. 109, 963–972. https://doi.org/10.1104/pp.109.3.963.

Vichi, M., 2022. An indicator of sea ice variability for the Antarctic marginal ice zone. Cryosphere 16, 4087–4106. https://doi.org/10.5194/tc-16-4087-2022.

Vichi, M., Ryan-Keogh, T.J., 2019. SCALExperiment - Spring Cruise, p. 2019.

Viljoen, J.J., Philibert, R., Van Horsten, N., Mtshali, T., Roychoudhury, A.N., Thomalla, S., Fietz, S., 2018. Phytoplankton response in growth, photophysiology and community structure to iron and light in the polar frontal zone and Antarctic waters. Deep Sea Res. Part Oceanogr. Res. Pap. 141, 118–129. https://doi.org/10.1016/j.dsr.2018.09.006.

Viljoen, J.J., Weir, I., Fietz, S., Cloete, R., Loock, J., Philibert, R., Roychoudhury, A.N., 2019. Links between the phytoplankton community composition and trace metal distribution in summer surface Waters of the Atlantic Southern Ocean. Front. Mar. Sci. 6, 295. https://doi.org/10.3389/fmars.2019.00295.

Wedepohl, K.H., 1995. The composition of the continental crust. Geochim. Cosmochim. Acta 59, 1217–1232. https://doi.org/10.1016/0016-7037(95)00038-2.

Welschmeyer, N.A., 1994. Fluorometric analysis of chlorophyll a in the presence of chlorophyll b and pheopigments. Limnol. Oceanogr. 39, 1985–1992. https://doi.org/10.4319/lo.1994.39.8.1985.

Westwood, K.J., Brian Griffiths, F., Meiners, K.M., Williams, G.D., 2010. Primary productivity off the Antarctic coast from 30°–80°E; BROKE-west survey, 2006. Deep Sea Res. Part II Top. Stud. Oceanogr. 57, 794–814. https://doi.org/10.1016/j.dsr2.2008.08.020.

Winter, A., Henderiks, J., Beaufort, L., Rickaby, R.E.M., Brown, C.W., 2014. Poleward expansion of the coccolithophore *Emiliania huxleyi*. J. Plankton Res. 36, 316–325. https://doi.org/10.1093/plankt/fbt110.

Wright, S.W., Ishikawa, A., Marchant, H.J., Davidson, A.T., Van Den Enden, R.L., Nash, G.V., 2009. Composition and significance of picophytoplankton in Antarctic waters. Polar Biol. 32, 797–808. https://doi.org/10.1007/s00300-009-0582-9.

Wright, S.W., Van Den Enden, R.L., Pearce, I., Davidson, A.T., Scott, F.J., Westwood, K.J., 2010. Phytoplankton community structure and stocks in the Southern Ocean (30–80°E) determined by CHEMTAX analysis of HPLC pigment signatures. Deep Sea Res. Part II Top. Stud. Oceanogr. 57, 758–778. https://doi.org/10.1016/j.dsr2.2009.06.015.

Xie, J., Bai, X., Lavoie, M., Lu, H., Fan, X., Pan, X., Fu, Z., Qian, H., 2015. Analysis of the proteome of the marine diatom *Phaeodactylum tricornutum* exposed to aluminum providing insights into aluminum toxicity mechanisms. Environ. Sci. Technol. 49, 11182–11190. https://doi.org/10.1021/acs.est.5b03272.

Yentsch, C.S., Yentsch, C.M., Phinney, D.A., Lapointe, B.E., Yentsch, S.F.W., 2004. The odyssey of new production. J. Exp. Mar. Biol. Ecol. 300, 15–30. https://doi.org/10.1016/j.jembe.2003.12.025.

Zapata, M., Jeffrey, S., Wright, S., Rodríguez, F., Garrido, J., Clementson, L., 2004. Photosynthetic pigments in 37 species (65 strains) of Haptophyta: implications for oceanography and chemotaxonomy. Mar. Ecol. Prog. Ser. 270, 83–102. https://doi.org/10.3354/meps270083.

Zhou, L., Liu, J., Xing, S., Tan, Y., Huang, L., 2018a. Phytoplankton responses to aluminum enrichment in the South China Sea. J. Inorg. Biochem. 181, 117–131. https://doi.org/10.1016/j.jinorgbio.2017.09.022.

Zhou, L., Tan, Y., Huang, L., Fortin, C., Campbell, P.G.C., 2018b. Aluminum effects on marine phytoplankton: implications for a revised Iron hypothesis (Iron–aluminum hypothesis). Biogeochemistry 139, 123–137. https://doi.org/10.1007/s10533-018-0458-6.

Zhou, L., Liu, F., Achterberg, E.P., Engel, A., Campbell, P.G.C., Fortin, C., Huang, L., Tan, Y., 2024. Promoting effects of aluminum addition on chlorophyll biosynthesis and growth of two cultured iron-limited marine diatoms. Limnol. Oceanogr. 69, 1157–1171. https://doi.org/10.1002/lno.12558.